



OPEN

## Dendrons containing boric acid and 1,3,5-tris(2-hydroxyethyl) isocyanurate covalently attached to silica-coated magnetite for the expeditious synthesis of Hantzsch esters

Mahsa Sam, Mohammad G. Dekamin✉ & Zahra Alirezvani

A new multifunctional dendritic nanocatalyst containing boric acid and 1,3,5-tris(2-hydroxyethyl) isocyanurate covalently attached to core-shell silica-coated magnetite ( $\text{Fe}_3\text{O}_4@\text{SiO}_2@\text{PTS-THEIC}-(\text{CH}_2)_3\text{OB}(\text{OH})_2$ ) was designed and properly characterized by different spectroscopic or microscopic methods as well as analytical techniques used for mesoporous materials. It was found that the combination of both aromatic  $\pi$ - $\pi$  stacking and boron-oxygen ligand interactions affords supramolecular arrays of dendrons. Furthermore, the use of boric acid makes this dendritic catalyst a good choice, from corrosion, recyclability and cost points of view. The catalytic activity of  $\text{Fe}_3\text{O}_4@\text{SiO}_2@\text{PTS-THEIC}-(\text{CH}_2)_3\text{OB}(\text{OH})_2$  as an efficient magnetically recoverable catalyst, was investigated for the synthesis of polyhydroacridines (PHAs) as well as polyhydroquinolines (PHQs) via one-pot multicomponent reactions of dimedone and/or ethyl acetoacetate, different aldehydes and ammonium acetate in EtOH under reflux conditions. Very low loading of the catalyst, high to quantitative yields of the desired PHAs or PHQs products, short reaction times, wide scope of the substrates, eliminating any toxic heavy metals or corrosive reagents for the modification of the catalyst, and simple work-up procedure are remarkable advantages of this green protocol. An additional advantage of this magnetic nanoparticles catalyst is its ability to be separated and recycled easily from the reaction mixture with minimal efforts in six subsequent runs without significant loss of its catalytic activity. This magnetic and dendritic catalyst can be extended to new two- and three-dimensional covalent organic frameworks with different applications.

New materials are required to be developed for the modern science and technology. These new materials are used for different applications such as drug delivery, medical diagnosis, reinforced composites, semiconductors, electronics, optics, sensors, sorbents,  $\text{CO}_2$  capture, heterogeneous catalysis, etc. In this manner, nanomaterials can play a vital role<sup>1-9</sup>. One of the emerging fields for the preparation and fabrication of new nanomaterials is dendrimer chemistry which has been recently expanded as two- or three-dimensional covalent organic frameworks (COFs). These strategies afford multifunctional materials which demonstrate synergistic effects and hence, higher performance and efficacy as well as newer and more specific properties than previous counterparts<sup>1,10-24</sup>. In addition, dendrimers can encapsulate and consequently, stabilize metallic catalytic active nanoparticles<sup>25-28</sup>. Furthermore, the properties of new materials can be modified and improved by their immobilization onto the surface of magnetic nanoparticles (MNPs), especially in the case of heterogeneous catalysis<sup>26,29-36</sup>. These improvements include better separation using an external magnetic field<sup>34,35,37-40</sup>, enhancement of the reaction rates by MNPs via local heating through induction and increasing the surface area as well as synergistic effects in conjunction with other catalytic species or centers due to the catalytic performance of magnetic materials, including Fe, Ni, Co or Ce-based ones<sup>41-43</sup>. Hence, active catalytic species or centres supported onto the surface

Pharmaceutical and Heterocyclic Compounds Research Laboratory, Department of Chemistry, Iran University of Science and Technology, 1684613114 Tehran, Iran. ✉email: mdekamin@iust.ac.ir

of MNPs have received much attention in the field of heterogeneous catalysis for promoting organic reactions in recent years<sup>26,44–46</sup>.

As a particular type of magnetic nanoparticles, superparamagnetic iron oxide nanoparticles (SPIONs) are more widely available than other MNPs due to advantages such as biologically well-accepted constituents, established size-selective preparation, diminished agglomeration, ease of preparation, and lower cost<sup>26,45,47–57</sup>. On the other hand, heterogenization of the active sites of usual dendritic catalysis has been pursued by either attaching the catalyst covalently within the dendrimer core or at the branch termini as well as through supramolecular interactions such as metal–ligand, hydrogen bonding, aromatic  $\pi$ – $\pi$  stacking, hydrophobic and van der Waals forces<sup>22,26,51,58–61</sup>. Therefore, design and preparation of new magnetic dendritic catalytic systems by appropriate application of dendron segments which can be expanded to 2D or 3D covalent organic frameworks (COFs) is still in high demand.

In recent years, thermally stable heteroaromatic 1,3,5-triazinane-2,4,6-trione (isocyanurate) moiety has received significant attention in polymer and material chemistry due to its numerous industrial applications, particularly in the field of low toxic drug-delivery agents, tensioactive building blocks and nonlinear optical properties, foams, surface coatings, films, paints, fibers, selective anion receptors and preparation of periodic mesoporous organosilica<sup>1,19,62–77</sup>. On the other hand, boric acid and its derivatives have achieved specific attention, as appropriate catalysts, in organic synthesis due to their advantages including high solubility in water, easy handling, low prices, and environmentally friendly and commercial availability<sup>78–87</sup>. In an attempt to indicate how applying SPIONs would affect the dendrimer bearing tridentate and thermally stable isocyanurate moiety as well as boric acid catalytic activity, this study reports the use of multifunctional dendritic nanocatalyst containing boric acid and 1,3,5-tris(2-hydroxyethyl)isocyanurate covalently attached to core–shell silica-coated SPIONs ( $\text{Fe}_3\text{O}_4@SiO_2@PTS\text{-THEIC}-(\text{CH}_2)_3\text{OB}(\text{OH})_2$ , **1**), as a novel and efficient supramolecular heterogeneous catalyst, in the one-pot synthesis of polyhydroacridines (PHAs, **5**) and polyhydroquinolines (PHQs, **7**) through multicomponent reaction (MCR) strategy (Scheme 1).

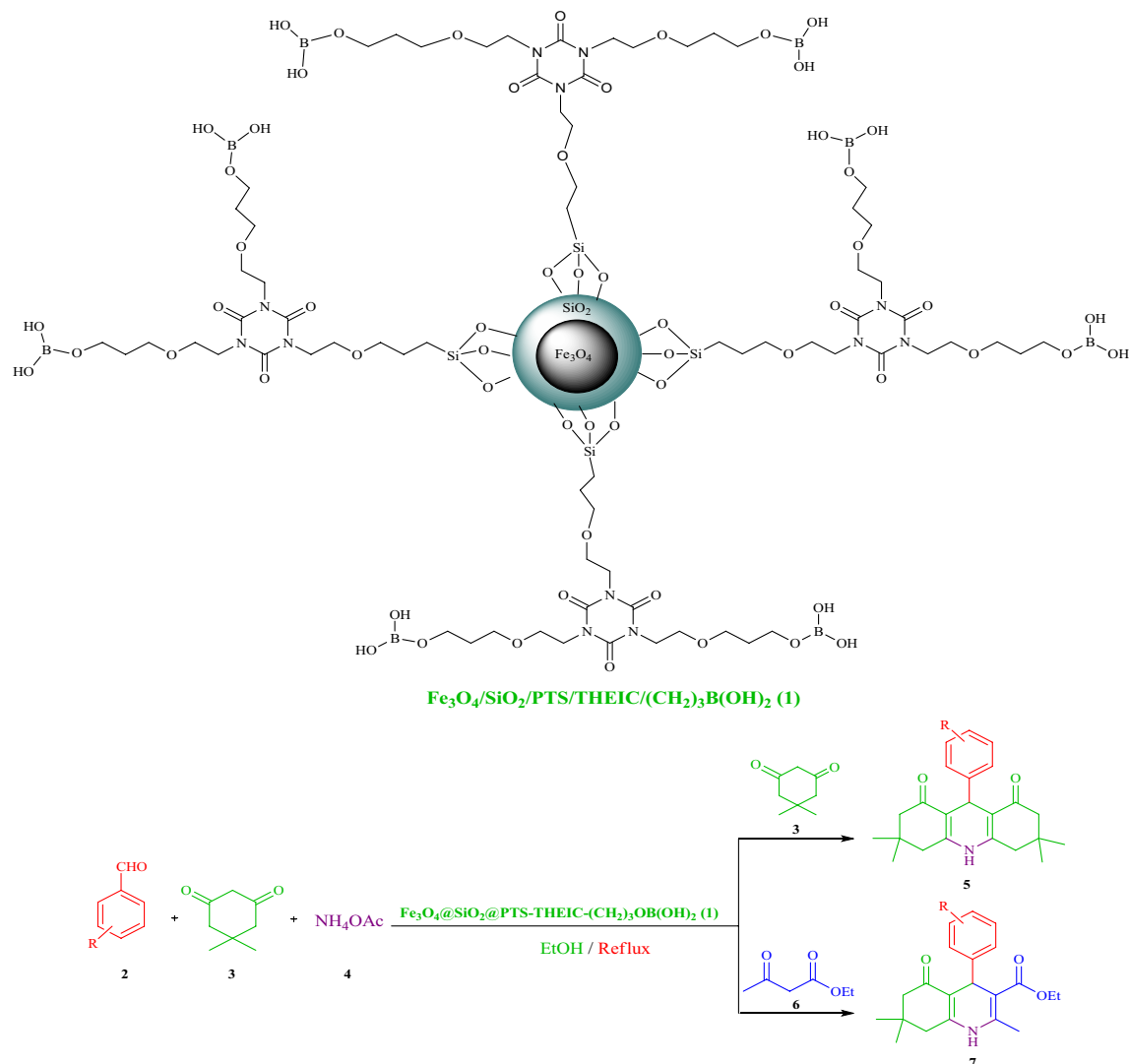
MCRs are one-pot reactions that involve more than two substrates demonstrating convergence as well as very high atom efficiency and bond-forming-index (BFI)<sup>88–90</sup>. Thus, MCRs are usually a good alternative for the sequential multistep synthesis, especially for useful heterocyclic scaffolds such as Hantzsch esters including 1,4-dihydropyridines (DHPs), PHQs and PHAs in organic synthesis and medicinal chemistry<sup>91–96</sup>. Generally known as one of the main groups of nitrogen heterocycles, polyhydroquinolines (PHQs) and polyhydroacridines (PHAs) have become considerably interesting due to their significant therapeutic and pharmacological properties<sup>97–100</sup>. Indeed, they are used as antimalaria, calcium  $\beta$ -blocker, antioxidant, antimicrobial, antifungal, vasodilator, anticancer, bronchodilator, antiatherosclerotic, geroprotective, hepatoprotective and antidiabetic agents as well as in the production of laser colors, radical reservoirs and safe hydrogen transfer agents<sup>4,101–111</sup>. First introduced by Arthur Hantzsch in 1882, Hantzsch reaction is an MCR that contains the combination of a  $\beta$ -dicarbonyl compound, an aldehyde and a source consisting of ammonia (usually  $\text{NH}_4\text{OAc}$ )<sup>112</sup>. However, catalytic systems are required to accelerate this multicomponent reaction. Here are some recent reported catalysts in this area: Mn@PMO-IL<sup>103</sup>, vanadium ion doped titania nanoparticles<sup>113</sup>, Lewis acidic mesoporous material (TUD-1) containing Fe<sup>114</sup>, magnetite nanoparticle-supported ceria<sup>41</sup>, silica-coated magnetic nanoparticles with tags of ionic liquid<sup>115</sup>, Boehmite silica sulfuric acid (Boehmite-SSA)<sup>116</sup>, PMO-ICSP $\text{rSO}_3\text{H}$ <sup>117</sup>,  $\text{Fe}_3\text{O}_4@B\text{-MCM-41}$ <sup>118</sup>, PS/PTSA<sup>119</sup>, PdRuNi@GO<sup>13</sup>, 1,3,5-tris(2-hydroxyethyl) isocyanurate covalently functionalized MCM-41<sup>120</sup>, alginic acid<sup>121,122</sup> and glycine nitrate ( $\text{GlyNO}_3$ ) ionic liquid<sup>123</sup>.

## Results and discussion

**Characterization of dendritic nanocatalyst containing boric acid and 1,3,5-tris(2-hydroxyethyl)isocyanurate covalently attached to core–shell silica-coated magnetite ( $\text{Fe}_3\text{O}_4@SiO_2@PTS\text{-THEIC}-(\text{CH}_2)_3\text{OB}(\text{OH})_2$ , **1**).** At first, the boric-acid-functionalized-1,3,5-tris(2-hydroxyethyl)isocyanurate attached to the silica-coated SPIONs ( $\text{Fe}_3\text{O}_4@SiO_2@PTS\text{-THEIC}-(\text{CH}_2)_3\text{OB}(\text{OH})_2$ , **1**) was characterized using different spectroscopic or analytical methods. As it has been shown in FT-IR spectrum (Fig. 1), the absorption bands at around 632 and 572  $\text{cm}^{-1}$  are related to the Fe–O bond vibrations. On the other hand, absorption band of Si–O–Si asymmetric stretching vibrations are apparent at around 1076  $\text{cm}^{-1}$ . Furthermore, the observed signals at 954, 802 and 459  $\text{cm}^{-1}$  are assigned to the symmetric stretching and bending vibrations of Si–O–Si bond<sup>43,57,124</sup>. Also, the absorption band of C=O bond vibrations of the isocyanurate moiety appeared at around 1637  $\text{cm}^{-1}$ <sup>177,120,125</sup>. Furthermore, the signals in range of 1350–1000  $\text{cm}^{-1}$  belong to the C–N bonds vibrations. On the other hand, the absorption band of B–O vibrations appeared at 1510  $\text{cm}^{-1}$ . Furthermore, there is an absorption signal at around 1191  $\text{cm}^{-1}$  which is related to B–O–H bond vibrations. Also, the signal at 563  $\text{cm}^{-1}$  is assigned to O–B–O bond vibrations. It is generally accepted that the broad band centred at 3400  $\text{cm}^{-1}$  is ascribed to the stretching vibrations of O–H bonds<sup>126,127</sup>. All of these data demonstrate that the catalyst **1** has been successfully prepared.

Energy dispersive spectroscopy (EDX) spectrum of  $\text{Fe}_3\text{O}_4@SiO_2@PTS\text{-THEIC}-(\text{CH}_2)_3\text{OB}(\text{OH})_2$  (**1**) proved that the magnetic catalyst functionalized with dendrons containing 1,3,5-tris(2-hydroxyethyl)isocyanurate and boric acid has been functionalized properly due to the presence of Fe, Si, O, C, N and B elements. The percentages of elements were measured to be B (1.96), C (6.99), N (2.50), O (63.58), Si (12.33) and Fe (12.65), respectively. It can be deduced from the absence of Cl and Br elements that terminal chloride groups of the 3-chloropropyl trimethoxysilane (3-APTS) linker as well as terminal bromide groups of the 1,3-dibromopropane linker have been completely replaced by covalent bonding (Fig. 2).

The X-ray diffraction (XRD) pattern of  $\text{Fe}_3\text{O}_4@SiO_2@PTS\text{-THEIC}-(\text{CH}_2)_3\text{OB}(\text{OH})_2$  (**1**) exhibited the phase structure and crystallization of the magnetic nanomaterials (Fig. 3). The main peaks were observed at  $2\theta$ : 27.9°, 32.5°, 33.8°, 55.6°, 56.4°, 62.3°. By comparing the XRD pattern of the prepared nanocatalyst (**1**) with the reference



**Scheme 1.** Schematic representation of the Fe<sub>3</sub>O<sub>4</sub>@SiO<sub>2</sub>@PTS-THEIC-(CH<sub>2</sub>)<sub>3</sub>OB(OH)<sub>2</sub> catalyst (1) and its catalytic activity in the one-pot synthesis of polyhydroacridines (5) and polyhydroquinolines (7) through multicomponent reaction (MCR) strategy (Drawn using the ChemDraw Ultra 12.0 software developed by PerkinElmer).

card numbers in the X<sup>3</sup>pert software, the crystal network of Fe<sub>3</sub>O<sub>4</sub>, SiO<sub>2</sub> and B(OH)<sub>3</sub> correspond with 072–2303, 082–1572 and 030–0199 card numbers, respectively.

The textural properties of the magnetic dendritic Fe<sub>3</sub>O<sub>4</sub>@SiO<sub>2</sub>@PTS-THEIC-(CH<sub>2</sub>)<sub>3</sub>OB(OH)<sub>2</sub> catalyst (1) was investigated by nitrogen adsorption–desorption isotherms (Fig. 4). The BET isotherm of the prepared catalyst corresponds with the BET standard type II adsorption isotherm. The surface area (BET), pore size and pore volume of the catalyst were calculated 55.8 m<sup>2</sup>/g, 13.9 nm, 0.19 cm<sup>3</sup>/g, respectively.

Thermal gravimetric analysis (TGA) and differential thermal analysis (DTA) measurements were carried out under air atmosphere by heating the sample at the rate of 10 °C min<sup>-1</sup> up to 800 °C (Fig. 5). The first weight loss under 100 °C is related to the removal of water and organic solvents which have remained in the dendritic catalyst through its preparation processes. On the other hand, the second weight loss about 150 °C can be assigned to the dehydration of boric acid moieties and their condensation. Furthermore, two distinct weight losses about 460 and 510 °C are attributed respectively to the decomposition of aliphatic linkers and 1,3,5-tris(2-hydroxyethyl) isocyanurate moieties in the structure of the dendritic Fe<sub>3</sub>O<sub>4</sub>@SiO<sub>2</sub>@PTS-THEIC-(CH<sub>2</sub>)<sub>3</sub>OB(OH)<sub>2</sub> catalyst (1) according to the data obtained by DTA (Fig. 5b).

Vibrating sample magnetometry (VSM) technique was used for measuring the magnetic properties of catalyst (1) at room temperature (Fig. 6). The saturation value of magnetization of Fe<sub>3</sub>O<sub>4</sub> and Fe<sub>3</sub>O<sub>4</sub>@SiO<sub>2</sub>@PTS-THEIC-(CH<sub>2</sub>)<sub>3</sub>OB(OH)<sub>2</sub> was measured to be 47.9 and 35.2 emu/g, respectively. Indeed, the reduction of saturation magnetization of Fe<sub>3</sub>O<sub>4</sub>@SiO<sub>2</sub>@PTS-THEIC-(CH<sub>2</sub>)<sub>3</sub>OB(OH)<sub>2</sub> shows that the dendritic catalyst has been formed. However, the observed saturation magnetization of catalyst (1) is enough and hence, it can be easily separated by an external magnetic field.



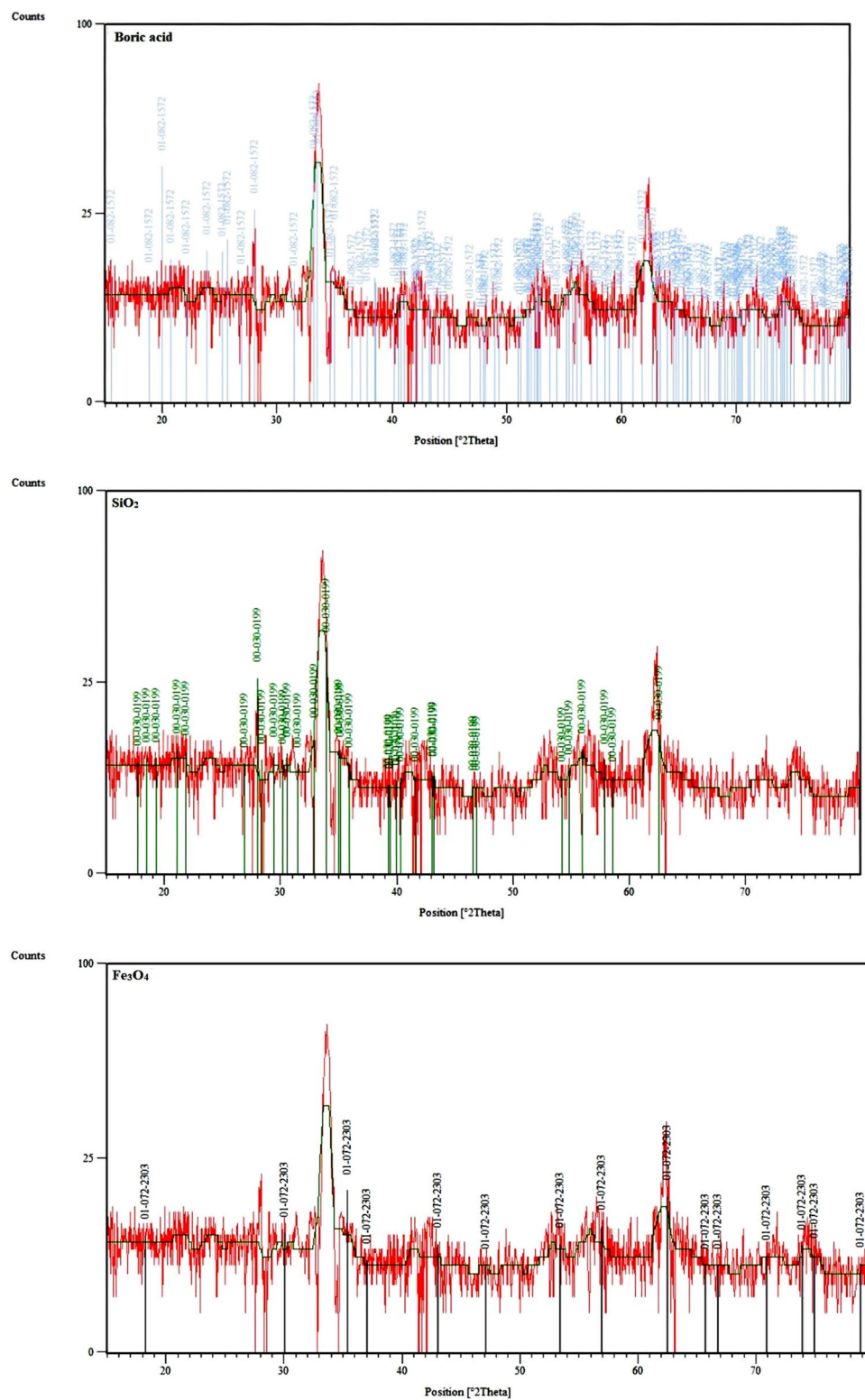


**Figure 3.** X-ray diffraction (XRD) pattern of the magnetic dendritic Fe<sub>3</sub>O<sub>4</sub>@SiO<sub>2</sub>@PTS-THEIC-(CH<sub>2</sub>)<sub>3</sub>OB(OH)<sub>2</sub> catalyst (**1**, the individual reference card numbers of the catalyst **1** components were collected from the X'pert HighScore Plus version 2.1 software developed by the PANalytical B.V.).

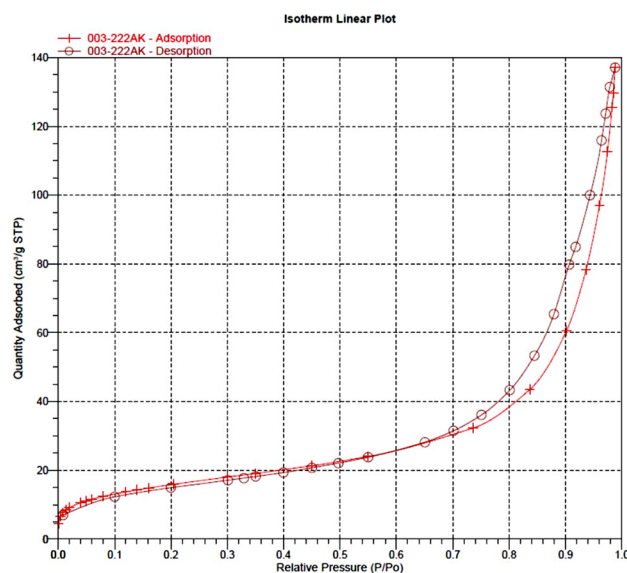


**Figure 4.** Nitrogen adsorption–desorption isotherm (BET) of the magnetic  $\text{Fe}_3\text{O}_4@SiO_2@PTS\text{-THEIC}-(\text{CH}_2)_3\text{OB(OH)}_2$  catalyst (**1**).

roquinoline-3-carboxylate (**7a**) were trace in the absence of any catalyst in EtOH at room temperature (entry 1). However, low yields of the desired products **5a** and **7a** were obtained under reflux conditions (entry 2) after long times. Interestingly, the yields were improved significantly in the presence of dendritic  $\text{Fe}_3\text{O}_4@SiO_2@PTS\text{-THEIC}-(\text{CH}_2)_3\text{OB(OH)}_2$  catalyst (**1**, entries 3–5). Further optimization of the reaction conditions illustrated that EtOH is the best solvent to promote the reaction with high efficiency for the synthesis of the desired products **5a** or **7a** (entries 6–12). The results of optimizing of the model reactions demonstrated that the optimal conditions for the reaction are 10 mg catalyst **1** loading in EtOH under reflux conditions. On the other hand, both boric acid and  $\text{Fe}_3\text{O}_4@SiO_2@PTS\text{-THEIC}$ , as the components of the catalyst **1**, afforded moderate yields of the desired products **5a** and **7a** at same catalyst loading under optimized conditions (entries 13 and 14). Finally, hot filtration test (the Sheldon test) was performed to prove the heterogeneous nature of the catalyst **1**. During this test, the solid catalyst **1** was removed from the mixture of model reaction for producing **7a** by filtration after 10 min using an external magnet. Then, the obtained mixture was heated again for 10 min. The result showed that after removal of the magnetic catalyst **1**, the model reaction did not proceed significantly. Indeed, only 48% of the desired product **7a** was isolated after 1 h (Fig. 8).

After finding the optimal conditions, the catalytic activity of  $\text{Fe}_3\text{O}_4@SiO_2@PTS\text{-THEIC}-(\text{CH}_2)_3\text{OB(OH)}_2$  nanocatalyst (**1**) was further expanded to several other aromatic or heterocyclic aldehydes for the synthesis of other derivatives of PHAs **5a–o** and PHQs **7a–u**. As it is shown in Tables 2 and 3, the isolated yields of the desired products **6** or **8** were good to excellent in all studied cases under the optimized condition of reaction. In most cases, the products were obtained in similar periods of time and yields compared to the model reaction. Indeed, aldehydes including aromatic carbocyclic or heterocyclic substrates well survived under optimized conditions without formation of any by-products. It is noteworthy that aldehydes bearing electron-withdrawing groups or six-membered heterocycles almost reacted faster than substrates having electron-donating groups or five-membered heterocycles. This trend of reactivity was observed in both symmetric and asymmetric Hantzsch reaction to afford PHAs **5a–o** or PHQs **7a–u** derivatives, respectively. Furthermore, the  $\alpha,\beta$ -unsaturated cinnamaldehyde (**2q**) or aliphatic butyraldehyde (**2r**) reacted in longer reaction times and afforded lower yields. These may be due to resonance and electron-releasing of the double bond and alkyl groups, respectively. All of these findings, led us to propose a plausible mechanism depicted in Scheme 2.

An important distinguishing feature of this magnetic dendritic nanocatalyst (**1**) beside easy separation from the reaction mixture is its recyclability. After the reaction was completed, the catalyst was separated and washed by acetone and hexane, respectively. Then, it was dried and reused in the model reactions for the next runs. The obtained results have been summarized in Fig. 9. These results show that this catalyst can be recovered and reused at least for five times in further runs under optimized conditions without a notable loss of its activity. Furthermore, comparison of the FTIR spectra of both fresh dendritic  $\text{Fe}_3\text{O}_4@SiO_2@PTS\text{-THEIC}-(\text{CH}_2)_3\text{OB(OH)}_2$  nanocatalyst (**1**) and the recycled sample after six consecutive runs for the synthesis of **5a** demonstrated that their structures are almost similar (Fig. 10).

Table 4 contains some of the formerly reported methods and representing their catalytic activity for the synthesis of polyhydroacridines and polyhydroquinolines to compare them with the dendritic  $\text{Fe}_3\text{O}_4@SiO_2@PTS\text{-THEIC}-(\text{CH}_2)_3\text{OB(OH)}_2$ . These data clearly demonstrate that the nanocatalyst **1** is more active than other previously reported catalytic systems in terms of catalyst loading, product yield, required reaction time and avoiding the toxic solvents.

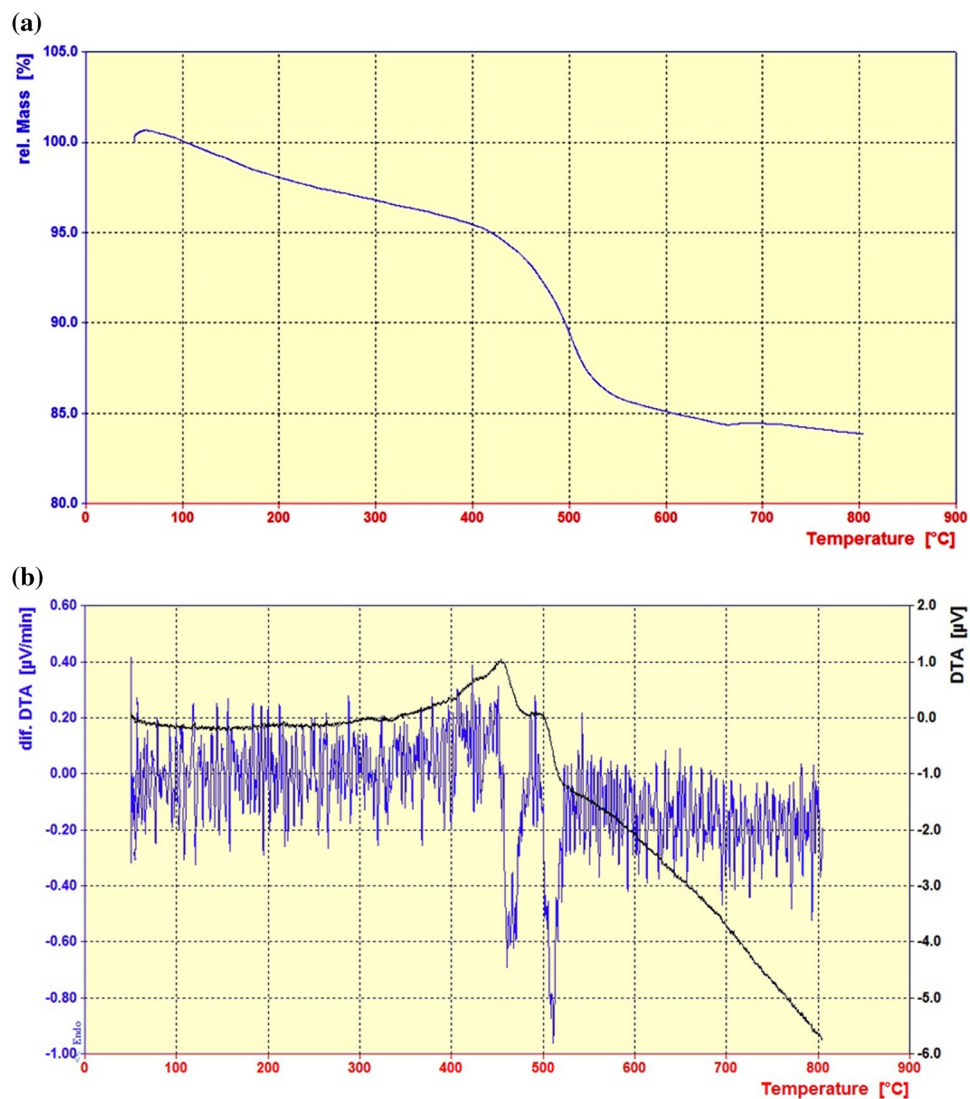


**Figure 5.** (a) Thermal gravimetric analysis (TGA) and (b) differential thermal analysis (DTA) curves of the magnetic dendritic  $\text{Fe}_3\text{O}_4@SiO_2@PTS\text{-THEIC}\text{-}(\text{CH}_2)_3\text{OB}(\text{OH})_2$  catalyst (1).

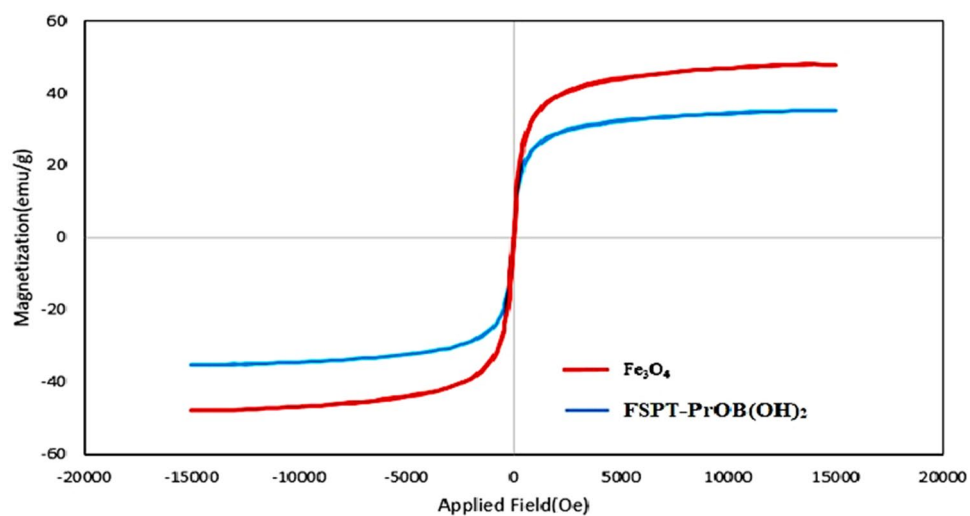


**Figure 6.** VSM analysis of the magnetic dendritic  $\text{Fe}_3\text{O}_4@SiO_2@PTS\text{-THEIC}\text{-}(\text{CH}_2)_3\text{OB}(\text{OH})_2$  catalyst (1, reproduced using the Microsoft Excel 2016).

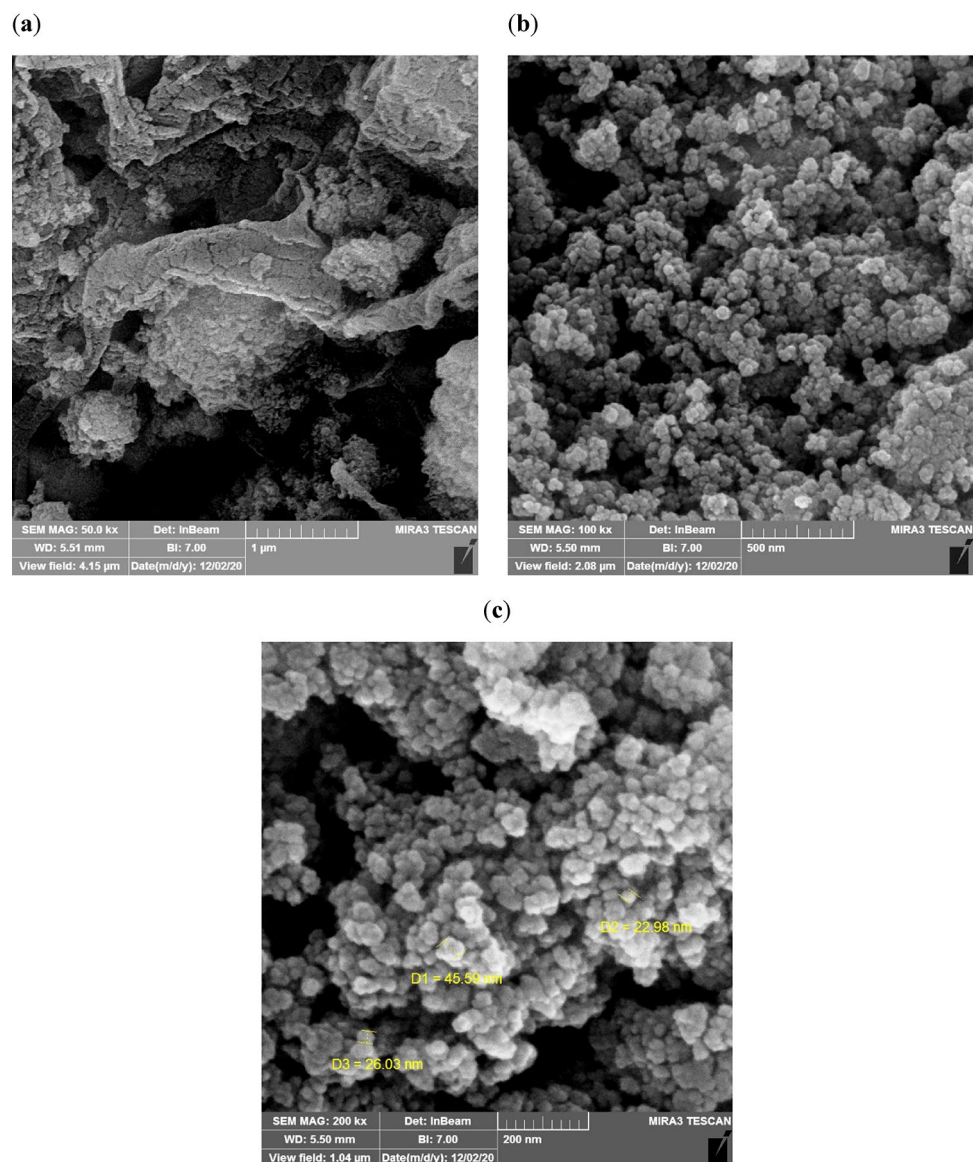


**Figure 7.** FESEM images of  $\text{Fe}_3\text{O}_4@SiO_2@PTS\text{-THEIC}\text{-}(\text{CH}_2)_3\text{OB(OH)}_2$  magnetically recoverable catalyst (**1**).

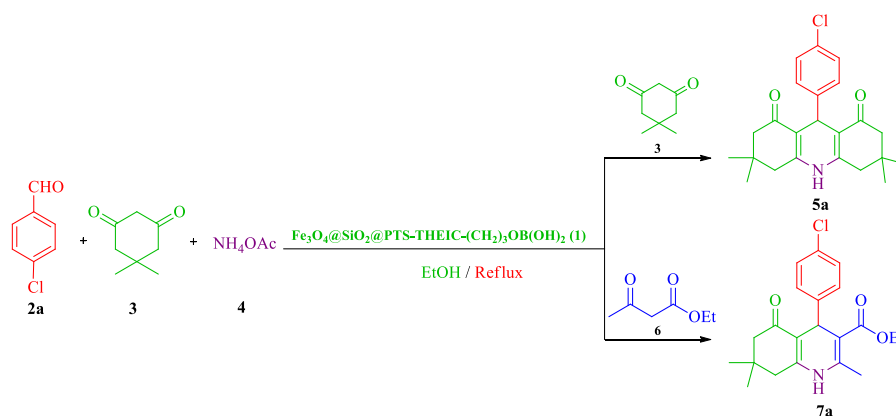
**Experimental section.** *General information.* All chemicals and reagents were provided by Merck or Aldrich chemical companies and used as received without any further purification, except for benzaldehyde which was used as a fresh distilled sample. FTIR spectra were recorded using KBr pellets on a Shimadzu FT IR-8400S spectrometer. Energy dispersive spectroscopy (EDS) was recorded on a SAMx instrument. The X-ray powder diffraction (XRD) data were collected on an X'Pert MPD Philips diffractometer with Cu radiation source ( $\lambda = 1.54050 \text{ \AA}$ ) at 40 kV voltage and 40 mA current. Field emission scanning electron microscopy (FESEM) images were obtained using a MIRA3 instrument of TESCAN Company, Czech Republic. Thermal gravimetric analysis (TGA) and differential thermal analysis (DTA) were performed by means of a Bahr company STA 504 instrument. The BET specific surface area of the catalyst **1** was obtained using an equipment ASAP 2020 Micromeritics. Magnetic susceptibility measurements were taken out by using a Lakeshore VSM, 7410 series. Melting points were determined using an Electrothermal 9100 apparatus and are uncorrected.  $^1\text{H}$  NMR (500 MHz) spectra were obtained using a Bruker DRX-500 AVANCE spectrometer in  $\text{CDCl}_3$  at ambient temperature. Analytical TLC was carried out using Merck 0.2 mm silica gel 60 F-254 Al-plates and n-hexane: EtOAc, (3:1, v/v %) as eluent. All products are known and their structures were established by comparing the physical constants as well as FTIR and NMR spectroscopic data with authentic samples<sup>120,122,141</sup>.

**Preparation of  $\text{Fe}_3\text{O}_4@SiO_2$  nanoparticles modified by (3-chloropropyl) trimethoxysilane ( $\text{Fe}_3\text{O}_4@SiO_2@CPTS$ ).** The  $\text{Fe}_3\text{O}_4@SiO_2@CPTS$  materials were prepared according to the reported methods in literature with a slight modification<sup>56</sup>.

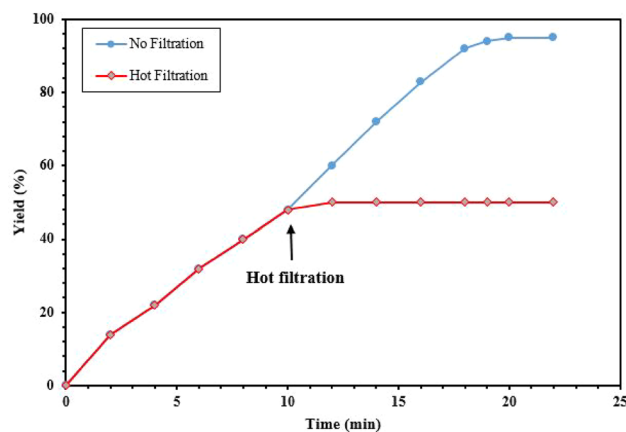


| Entry | Catalyst 1 loading (mg)  | Solvent            | Temp. (°C) | Time (min) | Yield <sup>b</sup> (%) Product 5a | Time (min) | Yield (%) Product 7a |
|-------|--|--------------------|------------|------------|-----------------------------------|------------|----------------------|
| 1     | –  | EtOH               | r.t        | 190        | Trace                             | 120        | Trace                |
| 2     | –  | EtOH               | Reflux     | 140        | 22                                | 100        | 25                   |
| 3     | 5  | EtOH               | Reflux     | 100        | 86                                | 45         | 85                   |
| 4     | 10   | EtOH               | Reflux     | 60         | 92                                | 20         | 95                   |
| 5     | 15   | EtOH               | Reflux     | 60         | 92                                | 20         | 95                   |
| 6     | 10   | H <sub>2</sub> O   | Reflux     | 110        | 67                                | 70         | 64                   |
| 7     | 10   | CH <sub>3</sub> CN | Reflux     | 115        | 78                                | 80         | 85                   |
| 8     | 10   | EtOH               | r.t        | 100        | 76                                | 90         | 80                   |
| 9     | 10   | H <sub>2</sub> O   | r.t        | 130        | 70                                | 100        | 64                   |
| 10    | 10   | EtOH               | 60 °C      | 90         | 84                                | 60         | 84                   |
| 11    | 10   | H <sub>2</sub> O   | 60 °C      | 120        | 70                                | 90         | 64                   |
| 12    | 10   | Solvent-Free       | 60 °C      | 100        | 82                                | 60         | 86                   |
| 13    | 10 (H <sub>3</sub> BO <sub>3</sub> )                             | EtOH               | Reflux     | 60         | 61                                | 20         | 66                   |
| 14    | 10 (Fe <sub>3</sub> O <sub>4</sub> @SiO <sub>2</sub> @PTS-THEIC) | EtOH               | Reflux     | 60         | 75                                | 20         | 78                   |

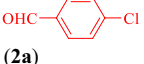
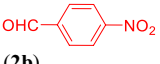
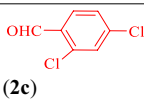
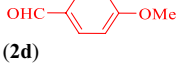
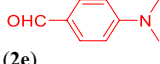
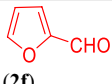
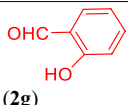
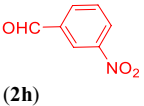
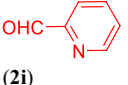
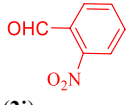
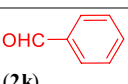
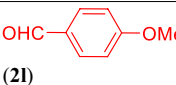
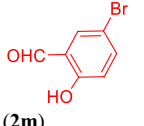
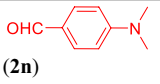
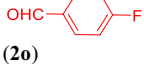
**Table 1.** Optimization of the reaction of 4-chlorobenzaldehyde (**2a**), dimedone (**3**), NH<sub>4</sub>OAc (**4**) and/or ethyl acetoacetate (**6**) under different conditions (The chemical structures were drawn using ChemDraw Ultra 12.0 software developed by PerkinElmer)<sup>a</sup>.



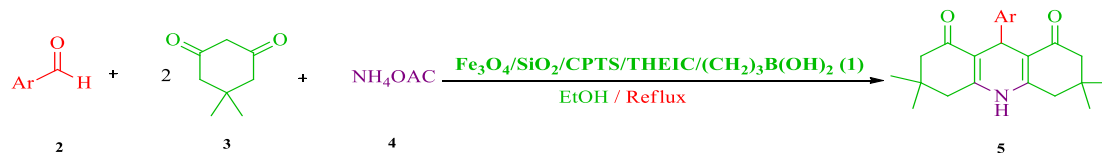
<sup>a</sup>Reaction conditions: 4-chlorobenzaldehyde (**2a**, 1 mmol), dimedone (**3**, 2 or 1 mmol), NH<sub>4</sub>OAc (**4**, 1.5 mmol) or ethyl acetoacetate (**6**, 1 mmol) in EtOH (2 ml); <sup>b</sup>isolated yields.



**Figure 8.** Hot filtration test for the synthesis of ethyl 4-(4-chlorophenyl)-2,7,7-trimethyl-5-oxo-1,4,5,6,7,8-hexahydroquinoline-3-carboxylate (**7a**) under optimized conditions (reproduced using the Microsoft Excel 2016).

| Entry | ArCHO 2   | Product 5 | Time (min) | Yield <sup>b</sup> % | Mp (°C) Obs [Lit.] <sup>c</sup>  |
|-------|---|-----------|------------|----------------------|----------------------------------|
| 1     | <br>(2a)   | 5a        | 60         | 92                   | 311–313 [315–317] <sup>129</sup> |
| 2     | <br>(2b)   | 5b        | 90         | 80                   | 197–200 [201–203] <sup>130</sup> |
| 3     | <br>(2c)   | 5c        | 75         | 80                   | 321–323 [321] <sup>131</sup>     |
| 4     | <br>(2d)   | 5d        | 45         | 93                   | 311–314 [311–313] <sup>131</sup> |
| 5     | <br>(2e)   | 5e        | 60         | 80                   | 308–310 [310–312] <sup>132</sup> |
| 6     | <br>(2f)   | 5f        | 60         | 85                   | 249–252 [249–251] <sup>133</sup> |
| 7     | <br>(2g)   | 5g        | 160        | 72                   | 220–223 [223–225] <sup>134</sup> |
| 8     | <br>(2h)   | 5h        | 90         | 87                   | 268–270 [273–275] <sup>130</sup> |
| 9     | <br>(2i)  | 5i        | 60         | 82                   | 284–286 [284–286] <sup>135</sup> |
| 10    | <br>(2j) | 5j        | 95         | 85                   | 280–282 [282–283] <sup>130</sup> |
| 11    | <br>(2k) | 5k        | 100        | 85                   | 244–246 [246–248] <sup>136</sup> |
| 12    | <br>(2l) | 5l        | 60         | 88                   | 301–303 [298–300] <sup>136</sup> |
| 13    | <br>(2m) | 5m        | 60         | 86                   | 328–330 [320–325] <sup>137</sup> |
| 14    | <br>(2n) | 5n        | 160        | 80                   | 277–279 [278–279] <sup>138</sup> |
| 15    | <br>(2o) | 5o        | 90         | 82                   | 272–274 [274–276] <sup>133</sup> |

**Table 2.**  $\text{Fe}_3\text{O}_4@/\text{SiO}_2@/\text{PTS-THEIC}-(\text{CH}_2)_3\text{OB}(\text{OH})_2$ -catalyzed one-pot synthesis of polyhydroacridines **5a–o** from different aldehydes (**2a–o**), dimedone (**3**) and  $\text{NH}_4\text{OAc}$  (**4**) under the optimized conditions (The chemical structures were drawn using ChemDraw Ultra 12.0 software developed by PerkinElmer)<sup>a</sup>.



<sup>a</sup>Reaction conditions: aldehyde (**2**, 1 mmol), dimedone (**3**, 2 mmol) and  $\text{NH}_4\text{OAc}$  (**4**, 1.5 mmol) in EtOH (2 ml); <sup>b</sup>isolated yields. <sup>c</sup>All products are known and their structures were established from their spectral data and melting points compared to authentic samples or literature values.

**Preparation of the dendritic  $\text{Fe}_3\text{O}_4@/\text{SiO}_2@/\text{CPTS}/\text{THEIC}$  nanomaterials.**  $\text{Fe}_3\text{O}_4@/\text{SiO}_2@/\text{CPTS}$  (1 g) was dispersed in toluene (30 ml) and KI (1.66 g) was added to the obtained mixture with the mechanical stirring at 80 °C for 1 h. Then,  $\text{K}_2\text{CO}_3$  (1.38 g) and tris-(2-hydroxyethyl)-1,3,5-triazinane-2,4,6-trione (1 g) were added to the mixture and it was heated under reflux conditions for 8 h. The obtained solid was filtered off and washed with EtOH (5 ml) and then dried in an oven for 2 h.

**Preparation of the dendritic  $\text{Fe}_3\text{O}_4@/\text{SiO}_2@/\text{PTS-THEIC}-(\text{CH}_2)_3\text{OB}(\text{OH})_2$  nanocatalyst (1).** A mixture of  $\text{Fe}_3\text{O}_4@/\text{SiO}_2@/\text{CPTS}/\text{THEIC}$  (1 g) and 1,3-dibromopropane ( $d = 1.98 \text{ g}\cdot\text{cm}^{-3}$ , 2 ml) was added to toluene (15 ml) and heated at 40 °C for 12 h. The obtained solid was filtered off, washed with toluene (5 ml) and then dried in a vacuum oven at 60 °C for 2 h. The as-prepared solid and  $\text{H}_3\text{BO}_3$  (1 g) were mixed in EtOH (30 ml) and the obtained mixture was stirred at room temperature for 18 h. After completion of the process, the obtained brown solid was filtered off and washed with EtOH (5 ml) on a Buchner funnel and then kept in a vacuum oven at 60 °C for 12 h. The complete procedure for the preparation of catalyst **1** has been represented in Scheme 3.

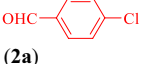
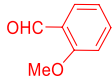
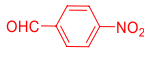
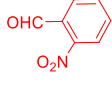
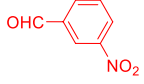
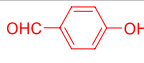
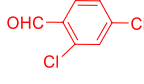
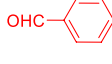
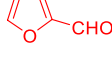
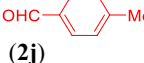
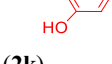
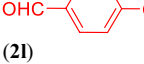
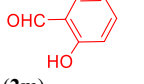
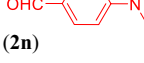
**General procedure for the synthesis of 1,8-dioxoacridindione derivatives **5a–o** catalyzed by magnetic dendritic  $\text{Fe}_3\text{O}_4@/\text{SiO}_2@/\text{PTS-THEIC}-(\text{CH}_2)_3\text{OB}(\text{OH})_2$  catalyst (1).** In a 5 mL round-bottomed flask, a mixture of aldehyde (**2a–o**, 1 mmol), dimedone (**3**, 2 mmol, 0.28 g),  $\text{NH}_4\text{OAc}$  (**4**, 1.5 mmol, 0.11 g) and  $\text{Fe}_3\text{O}_4@/\text{SiO}_2@/\text{PTS-THEIC}-(\text{CH}_2)_3\text{OB}(\text{OH})_2$  (**1**, 0.01 g) were added to EtOH 96% (2 mL). The obtained mixture was stirred under reflux conditions for the times indicated in Table 2. The progress of the reactions was monitored by TLC experiment (eluent; n-hexane: EtOAc, 3:1, v/v %). After completion of the reaction, EtOH (3 mL) was added to the mixture and it was heated to dissolve all organic compounds. Then, the catalyst **1** was easily separated by an external magnet and the solution was filtered. The filtrate was kept at room temperature and the crystals were collected by filtration to afford 1,8-dioxoacridindione derivatives **5a–o** in high purity.

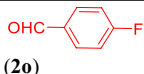
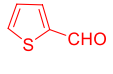
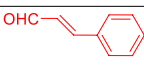
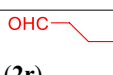
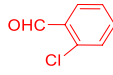
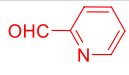
**General procedure for the synthesis of polyhydroquinoline derivatives **7a–u** catalyzed by magnetic dendritic  $\text{Fe}_3\text{O}_4@/\text{SiO}_2@/\text{PTS-THEIC}-(\text{CH}_2)_3\text{OB}(\text{OH})_2$  catalyst (1).** In a 5 mL round-bottomed flask, a mixture of aldehyde (**2a–u**, 1 mmol), dimedone (**3**, 1 mmol, 0.14 g),  $\text{NH}_4\text{OAc}$  (**4**, 1.5 mmol, 0.11 g), ethyl acetoacetate (**5**, 1 mmol, 0.13 g) and  $\text{Fe}_3\text{O}_4@/\text{SiO}_2@/\text{PTS-THEIC}-(\text{CH}_2)_3\text{OB}(\text{OH})_2$  (**1**, 0.01 g) were added to EtOH 96% (2 ml). The obtained mixture was stirred under reflux conditions for times indicated in Table 3. The progress of the reactions was monitored by TLC experiment (eluent; n-hexane: EtOAc, 3:1, v/v %). After completion of the reaction, EtOH (3 mL) was added to the mixture and it was heated to dissolve all organic compounds. Then, the catalyst **1** was easily separated by an external magnet and the solution was filtered. The filtrate was kept at room temperature and the crystals were collected by filtration to afford polyhydroquinoline derivatives **7a–u** in high purity.

**Selected spectral data.** 9-(4-Chlorophenyl)-3,3,6,6-tetramethyl-3,4,6,7,9,10-hexahydro-1,8(2H,5H)-acridindione (**5a**). Pale yellow solid; m.p. = 310–312 °C; FT-IR (KBr,  $\text{cm}^{-1}$ ): 3282, 3176, 3060, 2954, 2875, 1650, 1608, 1492, 1365, 1220, 1147, 1089, 1014, 840, 761, 597, 526; <sup>1</sup>H NMR (500 MHz,  $\text{CDCl}_3$ ):  $\delta$  (ppm): 0.98 (s, 6H, 2 $\text{CH}_3$ ), 1.10 (s, 6H, 2 $\text{CH}_3$ ), 2.19–2.37 (8H, m, 4 $\text{CH}_2$ ), 5.06 (s, 1H, CH), 7.17 (d, 2H, Ar-H), 7.28 (d, 2H, Ar-H), 6.97 (s, 1H, NH).

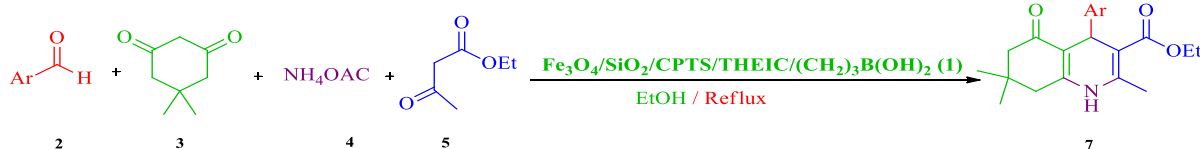
3,3,6,6-Tetramethyl-9-(pyridin-2-yl)-3,4,6,7,9,10-hexahydroacridine-1,8(2H,5H)-dione (**5i**): Pale yellow solid; m.p. = 284–286 °C; FT-IR (KBr,  $\text{cm}^{-1}$ ): 3604, 3519, 3440, 3284, 2875, 1637, 1600, 1477, 1365, 1218, 1139, 995, 744, 563; <sup>1</sup>H NMR (500 MHz,  $\text{CDCl}_3$ ):  $\delta$  (ppm): 0.98 (s, 6H, 2 $\text{CH}_3$ ), 1.07 (s, 6H, 2 $\text{CH}_3$ ), 2.12–2.46 (8H, m, 4 $\text{CH}_2$ ), 5.22 (s, 1H, CH), 7.51–7.58 (t, 3H, Ar-H), 8.41 (d, 1H, Ar-H), 6.97 (s, 1H, NH).

Ethyl 4-(4-methoxyphenyl)-2,7,7-trimethyl-5-oxo-1,4,5,6,7,8-hexahydroquinoline-3-carboxylate (**7l**). Pale yellow solid; mp.: 255–260 °C; FT-IR (KBr,  $\text{cm}^{-1}$ ): 3278, 3203, 3076, 2956, 1699, 1604, 1496, 1379, 1276, 1218, 1070, 1031, 842, 765, 536; <sup>1</sup>H NMR (500 MHz,  $\text{CDCl}_3$ ):  $\delta$  (ppm): 0.92 (s, 3H,  $\text{CH}_3$ ), 1.04 (s, 3H,  $\text{CH}_3$ ), 1.20 (t, 3H,  $J = 7.2 \text{ Hz}$ ,  $\text{CH}_3$  (OEt)), 2.11–2.28 (m, 4H,  $\text{CH}_2$ ), 2.33 (s, 3H,  $\text{CH}_3$ ), 3.71 (s, 3H,  $\text{OCH}_3$ ), 4.03–4.07 (q, 2H,  $J = 7.2 \text{ Hz}$ ,

| Entry     | ArCHO 2  | Product 7 | Time (min) | Yield <sup>b</sup> % | Mp (°C) Obs [Lit.] <sup>c</sup>  |
|-----------|--|-----------|------------|----------------------|----------------------------------|
| 1         | <br><b>(2a)</b>   | <b>7a</b> | 20         | 95                   | 243–245 [242–244] <sup>115</sup> |
| 2         | <br><b>(2b)</b>   | <b>7b</b> | 20         | 92                   | 249–251 [248–250] <sup>139</sup> |
| 3         | <br><b>(2c)</b>   | <b>7c</b> | 45         | 89                   | 234–236 [238–240] <sup>139</sup> |
| 4         | <br><b>(2d)</b>   | <b>7d</b> | 45         | 92                   | 196–198 [200–202] <sup>140</sup> |
| 5         | <br><b>(2e)</b>   | <b>7e</b> | 45         | 84                   | 182–184 [182–184] <sup>115</sup> |
| 6         | <br><b>(2f)</b>   | <b>7f</b> | 60         | 80                   | 224–226 [226–228] <sup>140</sup> |
| 7         | <br><b>(2g)</b>   | <b>7g</b> | 45         | 85                   | 234–237 [238–241] <sup>141</sup> |
| 8         | <br><b>(2h)</b> | <b>7h</b> | 45         | 96                   | 223–225 [224–226] <sup>115</sup> |
| 9         | <br><b>(2i)</b> | <b>7i</b> | 55         | 96                   | 235–237 [239–242] <sup>140</sup> |
| 10        | <br><b>(2j)</b> | <b>7j</b> | 25         | 93                   | 260–263 [263–265] <sup>115</sup> |
| 11        | <br><b>(2k)</b> | <b>7k</b> | 220        | 67                   | 209–212 [208–211] <sup>142</sup> |
| 12        | <br><b>(2l)</b> | <b>7l</b> | 20         | 95                   | 256–259 [255–257] <sup>115</sup> |
| 13        | <br><b>(2m)</b> | <b>7m</b> | 190        | 62                   | 223–225 [225–227] <sup>143</sup> |
| 14        | <br><b>(2n)</b> | <b>7n</b> | 80         | 70                   | 230–232 [233–235] <sup>144</sup> |
| Continued |  |           |            |                      |                                  |

| Entry | ArCHO 2   | Product 7 | Time (min) | Yield <sup>b</sup> % | Mp (°C) Obs [Lit.] <sup>c</sup>  |
|-------|---|-----------|------------|----------------------|----------------------------------|
| 15    | <br>(2o) | 7o        | 90         | 65                   | 186–188 [184–186] <sup>144</sup> |
| 16    | <br>(2p) | 7p        | 120        | 74                   | 218–221 [223–225] <sup>144</sup> |
| 17    | <br>(2q) | 7q        | 90         | 56                   | 203–20 [204–205] <sup>141</sup>  |
| 18    | <br>(2r) | 7r        | 90         | 67                   | 166–168 [165–167] <sup>145</sup> |
| 19    | <br>(2t) | 7t        | 55         | 94                   | 273–275 [274–276] <sup>146</sup> |
| 20    | <br>(2u) | 7u        | 45         | 80                   | 157–160 [157–160] <sup>147</sup> |

**Table 3.** Fe<sub>3</sub>O<sub>4</sub>@SiO<sub>2</sub>@PTS-THEIC-(CH<sub>2</sub>)<sub>3</sub>OB(OH)<sub>2</sub>-catalyzed one-pot synthesis of polyhydroquinolines 7a–u from different aldehydes (2a–u), dimedone (3), NH<sub>4</sub>OAc (4) and ethyl acetoacetate (5) under the optimized conditions (The chemical structures were drawn using ChemDraw Ultra 12.0 software developed by PerkinElmer)<sup>a</sup>.

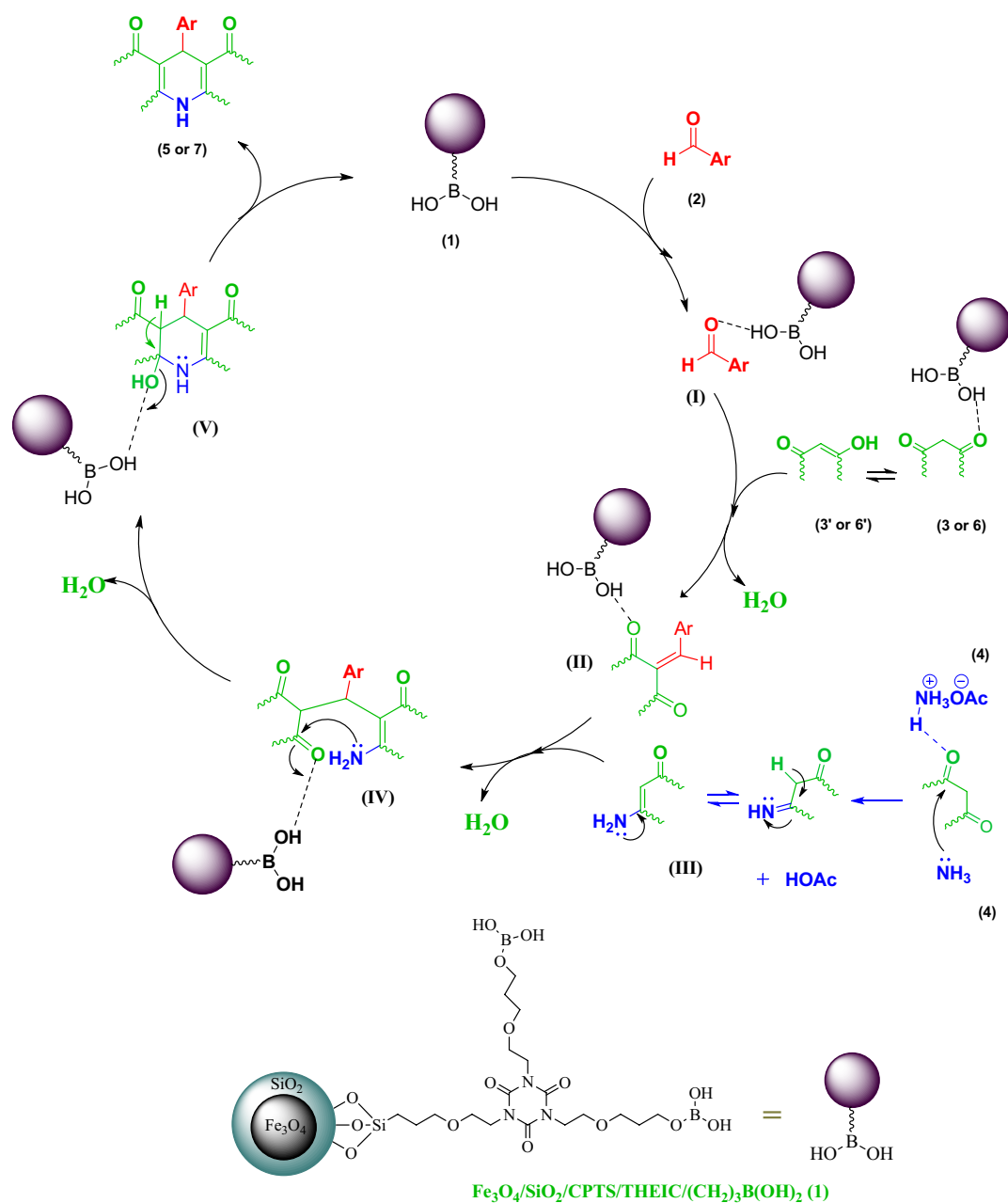


<sup>a</sup>Reaction conditions: aldehyde (2, 1 mmol), dimedone (3, 1 mmol), NH<sub>4</sub>OAc (4, 1.5 mmol) and ethyl acetoacetate (5, 1 mmol) in EtOH (2 ml); <sup>b</sup>isolated yields. <sup>c</sup>All products are known and their structures were established from their spectral data and melting points compared to authentic samples or literature values.

CH<sub>2</sub>(OEt), 4.98 (s, 1H, CH<sub>benzylic</sub>), 6.43 (br s, 1H, NH), 6.71–6.73 (d, 2H, *J* = 8.2 Hz, Ar–H), 7.21 (d, 2H, *J* = 8.2 Hz, Ar–H).

*Ethyl 2,7,7-trimethyl-4-(3-nitrophenyl)-5-oxo-1,4,5,6,7,8-hexahydroquinoline-3-carboxylate (7e)*. Pale yellow solid; m.p. = 180–184 °C; FT-IR (KBr, cm<sup>-1</sup>): 3276, 3193, 2964, 1703, 1604, 1490, 1379, 1278, 1215, 1143, 1070, 1022, 829, 754, 690, 507; <sup>1</sup>H NMR (500 MHz, CDCl<sub>3</sub>): δ (ppm): 0.93 (s, 3H, CH<sub>3</sub>), 1.09 (s, 3H, CH<sub>3</sub>), 1.19 (t, 3H, *J* = 7.2 Hz, CH<sub>3</sub>(OEt)), 2.13–2.40 (7H, s CH<sub>3</sub>, m 2CH<sub>2</sub>), 4.03–4.07 (q, 2H, *J* = 7.2 Hz, CH<sub>2</sub>(OEt)), 5.15 (s, 1H, CH<sub>benzylic</sub>), 5.98 (s, 1H, NH), 7.35–8.10 (m, 2H, Ar–H) (Supplementary Information 1).

**Conclusions.** In conclusion, the multifunctional dendritic nanocatalyst containing boric acid and 1,3,5-tris(2-hydroxyethyl)isocyanurate covalently attached to core-shell silica-coated magnetite (Fe<sub>3</sub>O<sub>4</sub>@SiO<sub>2</sub>@PTS-THEIC-(CH<sub>2</sub>)<sub>3</sub>OB(OH)<sub>2</sub>) was prepared and properly characterized for the first time. It was found that the combination of both aromatic π–π stacking and boron–oxygen ligand interactions affords supramolecular arrays of dendrons. The use of boric acid makes this dendritic catalyst a green choice from corrosion, recyclability and cost points of view. The magnetic dendritic catalyst was used, as a mild and recyclable catalyst, for the one-pot efficient synthesis of polyhydroacridines and polyhydroquinolines through MCR strategy in EtOH as a green solvent. Indeed, very low catalyst loading, short reaction times, mild reaction conditions, high to excellent yields, reusability of the catalyst, ease of separation by an external magnetic field, and the use of nontoxic materials for the preparation of the catalyst are among other advantages of this protocol. Further exploring of this magnetic dendritic magnetic catalyst for other organic transformations is underway in our research lab and would be presented in due course.



**Scheme 2.** Plausible mechanism for the one-pot synthesis of polyhydroacridines **5** and polyhydroquinolines **7** catalyzed by the agnetically recoverable  $\text{Fe}_3\text{O}_4/\text{SiO}_2/\text{PTS-THEIC}-(\text{CH}_2)_3\text{OB}(\text{OH})_2$  catalyst (**1**, Drawn using the ChemDraw Ultra 12.0 software developed by PerkinElmer).

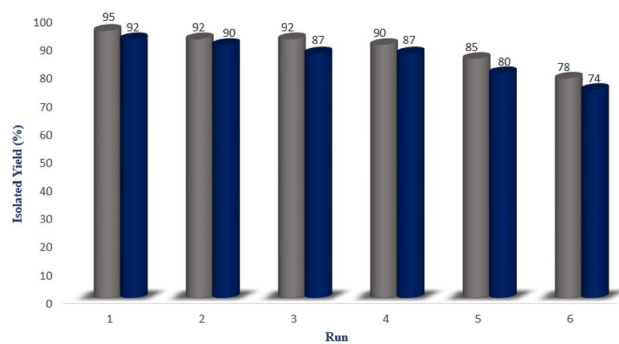


**Figure 9.** Recyclability of the dendritic  $\text{Fe}_3\text{O}_4@SiO_2@CPTS-THEIC-(CH_2)_3OB(OH)_2$  nanocatalyst (**1**) for the synthesis of **5a** and **7a** (Drawn using the Microsoft Excel 2016).

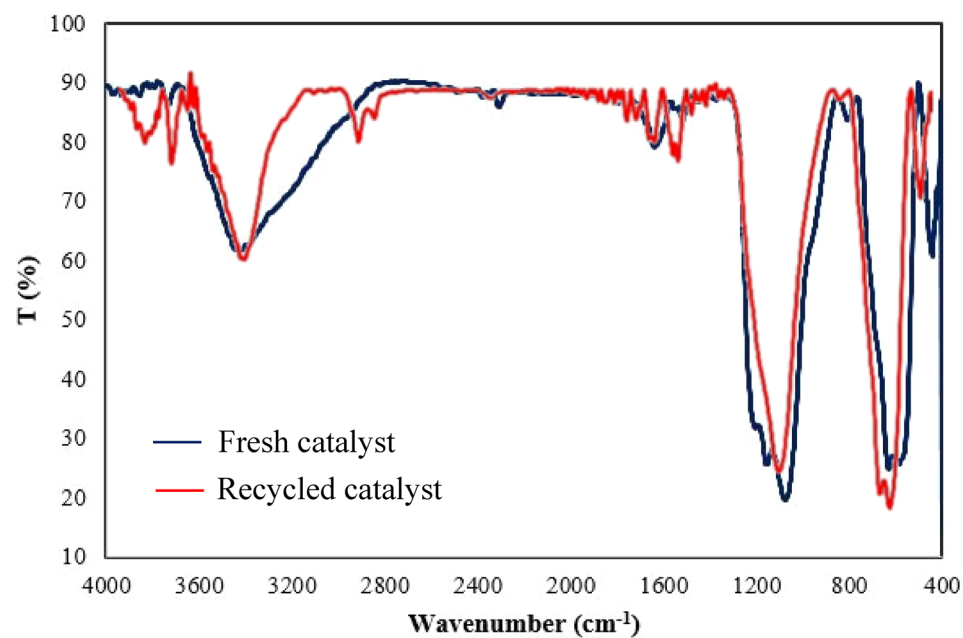
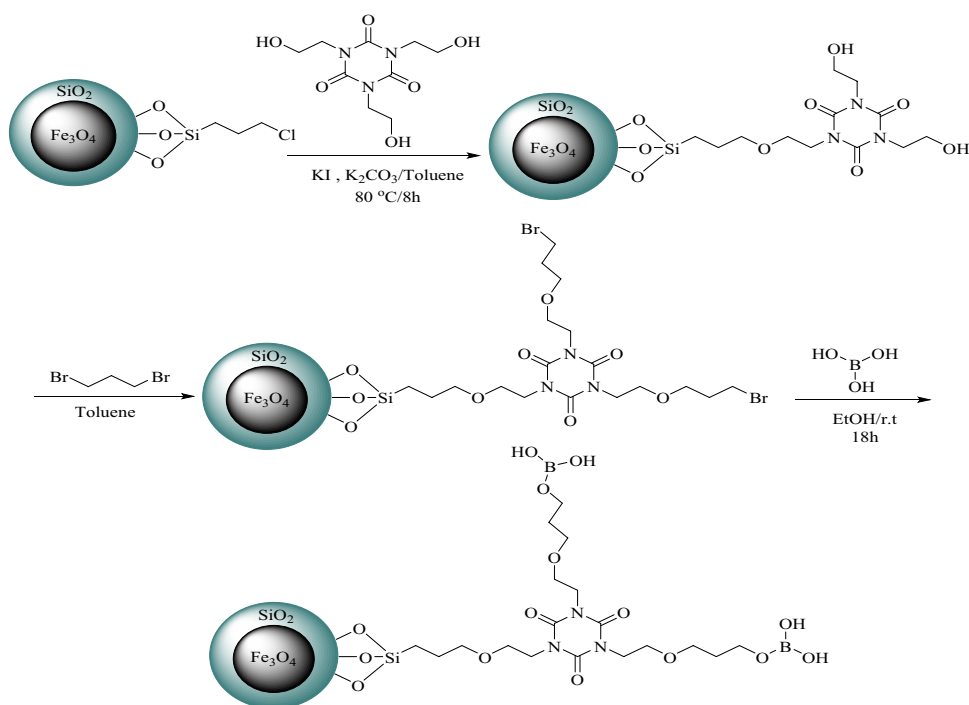


**Figure 10.** FTIR spectra of the fresh  $\text{Fe}_3\text{O}_4@SiO_2@CPTS-THEIC-(CH_2)_3OB(OH)_2$  nanocatalyst (**1**) and the recycled sample after six consecutive runs for the synthesis of **5a** (reproduced using the Microsoft Excel 2016).

| Entry | Catalyst  | Product | Catalyst Loading (mg) | Solvent               | T °C   | Time (min.) | Yield | Ref       |
|-------|---|---------|-----------------------|-----------------------|--------|-------------|-------|-----------|
| 1     | KH <sub>2</sub> PO <sub>4</sub>   | 5a      | 5 mol%                | EtOH/H <sub>2</sub> O | 120    | 5 h         | 94    | 146       |
| 2     | DABCO-PEG-400 ionic liquid  | 5a      | 80                    | –                     | 115    | 12–14 h     | 92    | 148       |
| 3     | Silica bonded <i>N</i> -propyl sulfamic acid  | 5a      | 30                    | EtOH                  | Reflux | 2 h         | 86    | 149       |
| 4     | Sawdust sulphonic acid  | 5a      | 50                    | EtOH                  | Reflux | 1 h         | 90    | 100       |
| 5     | Fe <sub>3</sub> O <sub>4</sub> @SiO <sub>2</sub> @PTS-THEIC-(CH <sub>2</sub> ) <sub>3</sub> OB(OH) <sub>2</sub> | 5a      | 10                    | EtOH                  | Reflux | 1 h         | 92    | This Work |
| 6     | L-proline   | 7a      | 10                    | EtOH                  | Reflux | 360         | 92    | 150       |
| 7     | Yb(OTf) <sub>3</sub>  | 7a      | 60                    | EtOH                  | 25     | 300         | 90    | 151       |
| 8     | PdRuNi@GO   | 7a      | 6                     | DMF                   | 70     | 45          | 92    | 24        |
| 9     | <i>p</i> -Toluenesulfonic acid  | 7a      | 18                    | –                     | r.t    | 120         | 90    | 152       |
| 10    | Fe <sub>3</sub> O <sub>4</sub> @B-MCM-41  | 7a      | 50                    | EtOH                  | Reflux | 40          | 92    | 118       |
| 11    | Silica Sulfuric Acid (SSA)  | 7a      | 80                    | –                     | 60     | 45          | 93    | 153       |
| 12    | PMO-ICS-PrSO <sub>3</sub> H   | 7a      | 20                    | EtOH                  | Reflux | 20          | 95    | 117       |
| 13    | Fe <sub>3</sub> O <sub>4</sub> @SiO <sub>2</sub> @PTS-THEIC-(CH <sub>2</sub> ) <sub>3</sub> OB(OH) <sub>2</sub> | 7a      | 10                    | EtOH                  | Reflux | 20          | 95    | This Work |

**Table 4.** Comparison of the synthesis of compounds **5a** and **7a** using the reported methods versus the present method.



**Scheme 3.** Schematic preparation of the dendritic Fe<sub>3</sub>O<sub>4</sub>@SiO<sub>2</sub>@PTS-THEIC-(CH<sub>2</sub>)<sub>3</sub>OB(OH)<sub>2</sub> catalyst (**1**), Drawn using the ChemDraw Ultra 12.0 software developed by PerkinElmer).

Received: 5 June 2020; Accepted: 30 December 2020

Published online: 27 January 2021

## References

- Guan, X., Chen, F., Fang, Q. & Qiu, S. Design and applications of three dimensional covalent organic frameworks. *Chem. Soc. Rev.* **49**, 1357–1384 (2020).
- Wood, J. The top ten advances in materials science. *Mater. Today* **11**, 40–45 (2008).
- Wu, J., Grimdale, A. C. & Müllen, K. Combining one-, two- and three-dimensional polyphenylene nanostructures. *J. Mater. Chem.* **15**, 41–52 (2005).
- Gu, F., Huang, W., Liu, X., Chen, W. & Cheng, X. Substituted hantzsch esters as versatile radical reservoirs in photoredox reactions. *Adv. Synth. Catal.* **360**, 925–931. <https://doi.org/10.1002/adsc.201701348> (2018).



5. Jiang, J. *et al.* Modularly constructed polyhedral oligomeric silsesquioxane-based giant molecules for unconventional nanostructure fabrication. *ACS Appl. Nano Mater.* **3**, 2952–2958. <https://doi.org/10.1021/acsnano.0c00231> (2020).
6. Xu, F. *et al.* Tunable superstructures of dendronized graphene nanoribbons in liquid phase. *J. Am. Chem. Soc.* **141**, 10972–10977. <https://doi.org/10.1021/jacs.9b04927> (2019).
7. Guo, C. *et al.* The potential of peptide dendron functionalized and gadolinium loaded mesoporous silica nanoparticles as magnetic resonance imaging contrast agents. *J. Mater. Chem. B* **4**, 2322–2331 (2016).
8. Ren, Y. & Xu, Q. Building close ties between CO<sub>2</sub> and functional two-dimensional nanomaterials with green chemistry strategy. *Energy Environ. Mater.* **1**, 46–60. <https://doi.org/10.1002/eem2.12005> (2018).
9. Han, T.-H., Kim, H., Kwon, S.-J. & Lee, T.-W. Graphene-based flexible electronic devices. *Mater. Sci. Eng. R Rep.* **118**, 1–43 (2017).
10. Tomalia, D. A., Christensen, J. B. & Boas, U. *Dendrimers, Dendrons, and Dendritic Polymers: Discovery, Applications, and the Future* (Cambridge University Press, Cambridge, 2012).
11. Sun, S. S. & Dalton, L. R. *Introduction to Organic Electronic and Optoelectronic Materials and Devices* (CRC Press, Boca Raton, 2016).
12. Buzzacchera, I. *et al.* Screening libraries of amphiphilic janus dendrimers based on natural phenolic acids to discover monodisperse unilamellar dendrimersomes. *Biomacromolecules* **20**, 712–727. <https://doi.org/10.1021/acs.biomac.8b01405> (2019).
13. Demirci, T. *et al.* One-pot synthesis of Hantzsch dihydropyridines using a highly efficient and stable PdRuNi@ GO catalyst. *RSC Adv* **6**, 76948–76956 (2016).
14. Svenson, S. The dendrimer paradox-high medical expectations but poor clinical translation. *Chem. Soc. Rev.* **44**, 4131–4144 (2015).
15. Newkome, G. R. & Shreiner, C. D. Poly(amidoamine), polypropylenimine, and related dendrimers and dendrons possessing different 1→2 branching motifs: An overview of the divergent procedures. *Polymer* **49**, 1–173. <https://doi.org/10.1016/j.polymer.2007.10.021> (2008).
16. Li, W., Huang, Y., Liu, Y., Tekell, M. C. & Fan, D. Three dimensional nanosuperstructures made of two-dimensional materials by design: Synthesis, properties, and applications. *Nano Today* **29**, 100799. <https://doi.org/10.1016/j.nantod.2019.100799> (2019).
17. Knights, K. A. *et al.* A rapid route to carbazole containing dendrons and phosphorescent dendrimers. *J. Mater. Chem.* **18**, 2121–2130. <https://doi.org/10.1039/B717750J> (2008).
18. Paez, J. I., Martinelli, M., Brunetti, V. & Strumia, M. C. Dendronization: A useful synthetic strategy to prepare multifunctional materials. *Polymers* **4**, 355–395 (2012).
19. Alahakoon, S. B., Diwakara, S. D., Thompson, C. M. & Smaldone, R. A. Supramolecular design in 2D covalent organic frameworks. *Chem. Soc. Rev.* **49**, 1344–1356 (2020).
20. El Kadib, A., Katir, N., Bousmina, M. & Majoral, J. P. Dendrimer–silica hybrid mesoporous materials. *New J. Chem.* **36**, 241–255 (2012).
21. Maity, A., Belgamwar, R. & Polshettiwar, V. Facile synthesis to tune size, textural properties and fiber density of dendritic fibrous nanosilica for applications in catalysis and CO<sub>2</sub> capture. *Nat. Protoc.* **14**, 2177 (2019).
22. Keller, M. *et al.* Pyrene-tagged dendritic catalysts noncovalently grafted onto magnetic Co/C nanoparticles: An efficient and recyclable system for drug synthesis. *Angew. Chem. Int. Ed.* **52**, 3626–3629. <https://doi.org/10.1002/anie.201209969> (2013).
23. Caminade, A.-M., Yan, D. & Smith, D. K. Dendrimers and hyperbranched polymers. *Chem. Soc. Rev.* **44**, 3870–3873 (2015).
24. Cui, W.-R. *et al.* Regenerable and stable sp<sup>2</sup> carbon-conjugated covalent organic frameworks for selective detection and extraction of uranium. *Nat Commun* **11**, 436. <https://doi.org/10.1038/s41467-020-14289-x> (2020).
25. Liu, X. *et al.* Precise localization of metal nanoparticles in dendrimer nanosnakes or inner periphery and consequences in catalysis. *Nat Commun* **7**, 1–8 (2016).
26. Wang, D., Deraedt, C., Ruiz, J. & Astruc, D. J. A. Magnetic and dendritic catalysts. *Acc. Chem. Res.* **48**, 1871–1880 (2015).
27. Deraedt, C., Pinaud, N. & Astruc, D. Recyclable catalytic dendrimer nanoreactor for part-per-million cui catalysis of “click” chemistry in water. *J. Am. Chem. Soc.* **136**, 12092–12098. <https://doi.org/10.1021/ja5061388> (2014).
28. Tarahomi, M., Alinezhad, H. & Maleki, B. Immobilizing Pd nanoparticles on the ternary hybrid system of graphene oxide, Fe<sub>3</sub>O<sub>4</sub> nanoparticles, and PAMAM dendrimer as an efficient support for catalyzing sonogashira coupling reaction. *Appl. Organomet. Chem.* **33**, e5203 (2019).
29. Nguyen, D.-V. *et al.* Mastering bioactive coatings of metal oxide nanoparticles and surfaces through phosphonate dendrons. *New J. Chem.* **44**, 3206–3214. <https://doi.org/10.1039/C9NJ05565G> (2020).
30. Qi, W. *et al.* An efficient magnetic carbon-based solid acid treatment for corn cob saccharification with high selectivity for xylose and enhanced enzymatic digestibility. *Green Chem.* **21**, 1292–1304 (2019).
31. Wei, X. W., Guo, G., Gong, C. Y., Gou, M. L. & Yong Qian, Z. *A Handbook of Applied Biopolymer Technology: Synthesis, Degradation and Applications* 365–387 (The Royal Society of Chemistry, London, 2011).
32. Grippin, A. J. *et al.* Dendritic cell-activating magnetic nanoparticles enable early prediction of antitumor response with magnetic resonance imaging. *ACS Nano* **13**, 13884–13898. <https://doi.org/10.1021/acsnano.9b05037> (2019).
33. Zhou, L., Gao, C. & Xu, W. Magnetic dendritic materials for highly efficient adsorption of dyes and drugs. *ACS Appl. Mater. Interfaces* **2**, 1483–1491. <https://doi.org/10.1021/am100114f> (2010).
34. Rossi, L. M., Costa, N. J. S., Silva, F. P. & Wojcieszak, R. Magnetic nanomaterials in catalysis: Advanced catalysts for magnetic separation and beyond. *Green Chem.* **16**, 2906–2933. <https://doi.org/10.1039/C4GC00164H> (2014).
35. Pasinszki, T. *et al.* Copper nanoparticles grafted on carbon microspheres as novel heterogeneous catalysts and their application for the reduction of nitrophenol and one-pot multicomponent synthesis of hexahydroquinolines. *New J. Chem.* **42**, 1092–1098 (2018).
36. Maleki, B., Reiser, O., Esmailnezhad, E. & Choi, H. J. SO<sub>3</sub>H-dendrimer functionalized magnetic nanoparticles (Fe<sub>3</sub>O<sub>4</sub>@DNH (CH<sub>2</sub>)<sub>4</sub>SO<sub>3</sub>H): Synthesis, characterization and its application as a novel and heterogeneous catalyst for the one-pot synthesis of polyfunctionalized pyrans and polyhydroquinolines. *Polyhedron* **162**, 129–141 (2019).
37. Hudson, R., Feng, Y., Varma, R. S. & Moores, A. Bare magnetic nanoparticles: sustainable synthesis and applications in catalytic organic transformations. *Green Chem.* **16**, 4493–4505 (2014).
38. Dalpozzo, R. J. G. C. Magnetic nanoparticle supports for asymmetric catalysts. *Green Chem.* **17**, 3671–3686 (2015).
39. Zolfigol, M. A. *et al.* A highly stable and active magnetically separable Pd nanocatalyst in aqueous phase heterogeneously catalyzed couplings. *Green Chem.* **15**, 2132–2140. <https://doi.org/10.1039/C3GC40421H> (2013).
40. Mohammadinezhad, A. & Akhlaghinia, B. Fe<sub>3</sub>O<sub>4</sub>@Boehmite-NH<sub>2</sub>-CoII NPs: an inexpensive and highly efficient heterogeneous magnetic nanocatalyst for the Suzuki-Miyaura and Heck-Mizoroki cross-coupling reactions. *Green Chem.* **19**, 5625–5641. <https://doi.org/10.1039/C7GC02647A> (2017).
41. Gawande, M. B. *et al.* Magnetically recyclable magnetite–ceria (Nanocat-Fe-Ce) nanocatalyst—applications in multicomponent reactions under benign conditions. *Green Chem.* **15**, 1226–1231. <https://doi.org/10.1039/C3GC40375K> (2013).
42. Koukabi, N. *et al.* Hantzsch reaction on free nano-Fe<sub>2</sub>O<sub>3</sub> catalyst: excellent reactivity combined with facile catalyst recovery and recyclability. *Chem. Commun.* **47**, 9230–9232. <https://doi.org/10.1039/C1CC12693H> (2011).
43. Akbari, A., Dekamin, M. G., Yaghoobi, A. & Naimi-Jamal, M. R. Novel magnetic propylsulfonic acid-anchored isocyanurate-based periodic mesoporous organosilica (Iron oxide@PMO-ICS-PrSO<sub>3</sub>H) as a highly efficient and reusable nanoreactor for the sustainable synthesis of imidazopyrimidine derivatives. *Sci. Rep.* **10**, 10646. <https://doi.org/10.1038/s41598-020-67592-4> (2020).

44. Chen, M.-N., Mo, L.-P., Cui, Z.-S. & Zhang, Z.-H. Magnetic nanocatalysts: Synthesis and application in multicomponent reactions. *Curr. Opin. Green Sustain. Chem.* **15**, 27–37 (2018).
45. Polshettiwar, V. *et al.* Magnetically recoverable nanocatalysts. *Chem. Rev.* **111**, 3036–3075. <https://doi.org/10.1021/cr100230z> (2011).
46. Nikoeei, N., Dekamin, M. G. & Valiey, E. Benzene-1,3,5-tricarboxylic acid-functionalized MCM-41 as a novel and recoverable hybrid catalyst for expeditious and efficient synthesis of 2,3-dihydroquinazolin-4(1H)-ones via one-pot three-component reaction. *Res. Chem. Intermed.* **46**, 3891–3909. <https://doi.org/10.1007/s11164-020-04179-8> (2020).
47. Mieloch, A. A., Żurawek, M., Giersig, M., Rozwadowska, N. & Rybka, J. D. Bioevaluation of superparamagnetic iron oxide nanoparticles (SPIONs) functionalized with dihexadecyl phosphate (DHP). *Sci. Rep.* **10**, 1–11 (2020).
48. Das, V. K. *et al.* Graphene derivative in magnetically recoverable catalyst determines catalytic properties in transfer hydrogenation of nitroarenes to anilines with 2-propanol. *ACS Appl. Mater. Interfaces* **10**, 21356–21364. <https://doi.org/10.1021/acscami.8b06378> (2018).
49. Mohammadi, R., Esmati, S., Gholamhosseini-Nazari, M. & Teimuri-Mofrad, R. Synthesis and characterization of a novel Fe<sub>3</sub>O<sub>4</sub>@SiO<sub>2</sub>-BenzIm-Fc [Cl]/BiOCl nano-composite and its efficient catalytic activity in the ultrasound-assisted synthesis of diverse chromene analogs. *New J. Chem.* **43**, 135–145 (2019).
50. Abu-Reziq, R., Alper, H., Wang, D. & Post, M. L. Metal supported on dendronized magnetic nanoparticles: Highly selective hydroformylation catalysts. *J. Am. Chem. Soc.* **128**, 5279–5282. <https://doi.org/10.1021/ja060140u> (2006).
51. Kainz, Q. M. & Reiser, O. Polymer- and dendrimer-coated magnetic nanoparticles as versatile supports for catalysts, scavengers, and reagents. *Acc. Chem. Res.* **47**, 667–677. <https://doi.org/10.1021/ar400236y> (2014).
52. Cheng, T., Zhang, D., Li, H. & Liu, G. Magnetically recoverable nanoparticles as efficient catalysts for organic transformations in aqueous medium. *Green Chem.* **16**, 3401–3427. <https://doi.org/10.1039/C4GC00458B> (2014).
53. Deng, Y., Qi, D., Deng, C., Zhang, X. & Zhao, D. Superparamagnetic high-magnetization microspheres with an Fe<sub>3</sub>O<sub>4</sub>@SiO<sub>2</sub> core and perpendicularly aligned mesoporous SiO<sub>2</sub> shell for removal of microcystins. *J. Am. Chem. Soc.* **130**, 28–29 (2008).
54. Heitsch, A. T., Smith, D. K., Patel, R. N., Ress, D. & Korgel, B. A. Multifunctional particles: Magnetic nanocrystals and gold nanorods coated with fluorescent dye-doped silica shells. *J. Solid State Chem.* **181**, 1590–1599. <https://doi.org/10.1016/j.jssc.2008.05.002> (2008).
55. Alirezvani, Z., Dekamin, M. G. & Valiey, E. Cu(II) and magnetite nanoparticles decorated melamine-functionalized chitosan: A synergistic multifunctional catalyst for sustainable cascade oxidation of benzyl alcohols/Knoevenagel condensation. *Sci Rep.* **9**, 17758. <https://doi.org/10.1038/s41598-019-53765-3> (2019).
56. Ishani, M., Dekamin, M. G. & Alirezvani, Z. Superparamagnetic silica core-shell hybrid attached to graphene oxide as a promising recoverable catalyst for expeditious synthesis of TMS-protected cyanohydrins. *J. Colloid Interface Sci.* **521**, 232–241. <https://doi.org/10.1016/j.jcis.2018.02.060> (2018).
57. Karami, S., Dekamin, M. G., Valiey, E. & Shakib, P. DABA MNPs: A new and efficient magnetic bifunctional nanocatalyst for the green synthesis of biologically active pyrano[2,3-c]pyrazole and benzylpyrazolyl coumarin derivatives. *New J. Chem.* **44**, 13952–13961. <https://doi.org/10.1039/D0NJ02666B> (2020).
58. Deng, J.-H. *et al.*  $\pi$ - $\pi$  stacking interactions: Non-negligible forces for stabilizing porous supramolecular frameworks. *Sci Adv.* **6**, 9976. <https://doi.org/10.1126/sciadv.aax9976> (2020).
59. Ulbrich, K. *et al.* Targeted drug delivery with polymers and magnetic nanoparticles: Covalent and noncovalent approaches, release control, and clinical studies. *Chem. Rev.* **116**, 5338–5431. <https://doi.org/10.1021/acs.chemrev.5b00589> (2016).
60. Sun, Z., Li, H., Cui, G., Tian, Y. & Yan, S. Multifunctional magnetic core-shell dendritic mesoporous silica nanospheres decorated with tiny Ag nanoparticles as a highly active heterogeneous catalyst. *Appl. Surf. Sci.* **360**, 252–262. <https://doi.org/10.1016/j.apsusc.2015.11.013> (2016).
61. Bronstein, L. M. Magnetically recoverable catalysts with dendritic ligands for enhanced catalysis and easy separation. *Chem-CatChem* **7**, 1058–1060. <https://doi.org/10.1002/cctc.201500007> (2015).
62. Li, C., Zhao, W., He, J. & Zhang, Y. Highly efficient cyclotrimerization of isocyanates using N-heterocyclic olefins under bulk conditions. *Chem. Commun.* **55**, 12563–12566. <https://doi.org/10.1039/C9CC06402H> (2019).
63. Guo, Z., Xu, Y., Wu, X., Wei, X. & Xi, C. Potassium complexes containing bidentate pyrrole ligands: synthesis, structures, and catalytic activity for the cyclotrimerization of isocyanates. *Dalton Trans.* **48**, 8116–8121. <https://doi.org/10.1039/C9DT01246J> (2019).
64. Liu, D., Zhou, D., Yang, H., Li, J. & Cui, C. Yttrium dialkyl supported by a silaamidinate ligand: synthesis, structure and catalysis on cyclotrimerization of isocyanates. *Chem. Commun.* **55**, 12324–12327. <https://doi.org/10.1039/C9CC06282C> (2019).
65. Lin, D., Luo, M., Lin, C., Xu, F. & Ye, N. KLi(HC<sub>3</sub>N<sub>3</sub>O<sub>3</sub>)<sub>2</sub>H<sub>2</sub>O: Solvent-drop grinding method toward the hydro-isocyanurate nonlinear optical crystal. *J. Am. Chem. Soc.* **141**, 3390–3394. <https://doi.org/10.1021/jacs.8b13280> (2019).
66. Lowinger, M. B., Barrett, S. E., Zhang, F. & Williams, R. O. Sustained release drug delivery applications of polyurethanes. *Pharmaceutics* **10**, 55 (2018).
67. Argouarch, G. *et al.* Triaryl-1,3,5-triazinane-2,4,6-triones (Isocyanurates) peripherally functionalized by donor groups: Synthesis and study of their linear and nonlinear optical properties. *Chemistry A European Journal* **18**, 11811–11827. <https://doi.org/10.1002/chem.201200484> (2012).
68. Moritsugu, M., Sudo, A. & Endo, T. Development of high-performance networked polymers consisting of isocyanurate structures based on selective cyclotrimerization of isocyanates. *J. Polym. Sci. Part A Polym. Chem.* **49**, 5186–5191. <https://doi.org/10.1002/pola.24987> (2011).
69. Raders, S. M. & Verkade, J. G. An electron-rich proazaphosphatrane for isocyanate trimerization to isocyanurates. *J. Org. Chem.* **75**, 5308–5311. <https://doi.org/10.1021/jo9023396> (2010).
70. Di, Y. & Heath, R. J. Collagen stabilization and modification using a polyepoxide, triglycidyl isocyanurate. *Polym. Degrad. Stab.* **94**, 1684–1692. <https://doi.org/10.1016/j.polymdegradstab.2009.06.019> (2009).
71. Pokladek, Z. *et al.* Linear and third-order nonlinear optical properties of triazobenzene-1,3,5-triazinane-2,4,6-trione (isocyanurate) derivatives. *ChemPlusChem* **82**, 1372–1383. <https://doi.org/10.1002/cplu.201700396> (2017).
72. Singh, H. & Jain, A. K. Ignition, combustion, toxicity, and fire retardancy of polyurethane foams: A comprehensive review. *J. Appl. Polym. Sci.* **111**, 1115–1143. <https://doi.org/10.1002/app.29131> (2009).
73. Gama, N. V., Ferreira, A. & Barros-Timmons, A. Polyurethane foams: Past, present, and future. *Materials* **11**, 1841 (2018).
74. Gale, P. A., Garcia-Garrido, S. E. & Garric, J. Anion receptors based on organic frameworks: Highlights from 2005 and 2006. *Chem. Soc. Rev.* **37**, 151–190. <https://doi.org/10.1039/B715825D> (2008).
75. Hettche, F. & Hoffmann, R. W. A tri-armed sulfonamide host for selective binding of chloride. *New J. Chem.* **27**, 172–177. <https://doi.org/10.1039/B206125M> (2003).
76. Olkhovik, O. & Jaroniec, M. Periodic mesoporous organosilica with large heterocyclic bridging groups. *J. Am. Chem. Soc.* **127**, 60–61. <https://doi.org/10.1021/ja043941a> (2005).
77. Zebardasti, A., Dekamin, M. G., Doustkhah, E. & Assadi, M. H. N. Carbamate-isocyanurate-bridged periodic mesoporous organosilica for van der Waals CO<sub>2</sub> capture. *Inorg. Chem.* **59**, 11223–11227. <https://doi.org/10.1021/acs.inorgchem.0c01449> (2020).
78. Hansen, T. S., Mielby, J. & Riisager, A. Synergy of boric acid and added salts in the catalytic dehydration of hexoses to 5-hydroxymethylfurfural in water. *Green Chem.* **13**, 109–114. <https://doi.org/10.1039/C9CG00355G> (2011).

79. Bhattacharyya, D. *et al.* Boric acid catalyzed chemoselective reduction of quinolines. *Org. Biomol. Chem.* **18**, 1214–1220. <https://doi.org/10.1039/C9OB02673H> (2020).
80. Pal, R. Boric acid in organic synthesis: scope and recent developments. *ARKIVOC Online J. Org. Chem.* **2018**, 346–371 (2018).
81. Chatterjee, M., Ishizaka, T., Suzuki, T., Suzuki, A. & Kawanami, H. In situ synthesized Pd nanoparticles supported on B-MCM-41: An efficient catalyst for hydrogenation of nitroaromatics in supercritical carbon dioxide. *Green Chem.* **14**, 3415–3422. <https://doi.org/10.1039/C2GC36160D> (2012).
82. Brun, E. *et al.* Microwave-assisted condensation reactions of acetophenone derivatives and activated methylene compounds with aldehydes catalyzed by boric acid under solvent-free conditions. *Molecules* **20**, 11617–11631 (2015).
83. Houston, T. A., Wilkinson, B. L. & Blanchfield, J. T. Boric acid catalyzed chemoselective esterification of  $\alpha$ -hydroxycarboxylic acids. *Org. Lett.* **6**, 679–681. <https://doi.org/10.1021/ol036123g> (2004).
84. Halimehjnai, A. Z., Hosseini, S., Gholami, H. & Hashemi, M. M. Boric acid/glycerol as an efficient catalyst for synthesis of thiomorpholine 1,1-dioxide by double Michael addition reaction in water. *Synth. Commun.* **43**, 191–197. <https://doi.org/10.1080/00397911.2011.594930> (2013).
85. Kumar, A. & Maurya, R. A. An unusual Mannich type reaction of tertiary aromatic amines in aqueous micelles. *Tetrahedron Lett.* **49**, 5471–5474. <https://doi.org/10.1016/j.tetlet.2008.07.019> (2008).
86. Dekamin, M. G., Mokhtari, Z. & Karimi, Z. Nano-ordered B-MCM-41: An efficient and recoverable solid acid catalyst for three-component Strecker reaction of carbonyl compounds, amines and TMSCN. *Sci. Iran.* **18**, 1356–1364. <https://doi.org/10.1016/j.scient.2011.11.005> (2011).
87. Yarhosseini, M., Javanshir, S., Dolatkah, Z. & Dekamin, M. G. An improved solvent-free synthesis of flunixin and 2-(arylamino) nicotinic acid derivatives using boric acid as catalyst. *Chem. Cent. J.* **11**, 124. <https://doi.org/10.1186/s13065-017-0355-4> (2017).
88. Cioc, R. C., Ruijter, E. & Orru, R. V. A. Multicomponent reactions: advanced tools for sustainable organic synthesis. *Green Chem.* **16**, 2958–2975. <https://doi.org/10.1039/C4GC00013G> (2014).
89. Paul, B., Maji, M., Chakrabarti, K. & Kundu, S. Tandem transformations and multicomponent reactions utilizing alcohols following dehydrogenation strategy. *Org. Biomol. Chem.* <https://doi.org/10.1039/C9OB02760B> (2020).
90. Huang, B., Zeng, L., Shen, Y. & Cui, S. One-pot multicomponent synthesis of  $\beta$ -amino amides. *Angew. Chem. Int. Ed.* **56**, 4565–4568 (2017).
91. Leonardi, M., Villacampa, M. & Menéndez, J. C. Multicomponent mechanochemical synthesis. *Chem. Sci.* **9**, 2042–2064. <https://doi.org/10.1039/C7SC05370C> (2018).
92. Martins, P. *et al.* Heterocyclic anticancer compounds: recent advances and the paradigm shift towards the use of nanomedicine's tool box. *Molecules* **20**, 16852–16891 (2015).
93. Gomtsyan, A. Heterocycles in drugs and drug discovery. *Chem. Heterocycl. Compd.* **48**, 7–10 (2012).
94. Dömling, A., Wang, W. & Wang, K. Chemistry and biology of multicomponent reactions. *Chem. Rev.* **112**, 3083–3135. <https://doi.org/10.1021/cr100233r> (2012).
95. Dekamin, M. G., Azimoshan, M. & Ramezani, L. Chitosan: A highly efficient renewable and recoverable bio-polymer catalyst for the expeditious synthesis of  $\alpha$ -amino nitriles and imines under mild conditions. *Green Chem.* **15**, 811–820. <https://doi.org/10.1039/C3GC36901C> (2013).
96. Dekamin, M. G. & Eslami, M. Highly efficient organocatalytic synthesis of diverse and densely functionalized 2-amino-3-cyano-4H-pyran under mechanochemical ball milling. *Green Chem.* **16**, 4914–4921. <https://doi.org/10.1039/C4GC00411F> (2014).
97. Mathew, G., Lincy, J. & Chippy, J. Synthesis, characterization and biological screening of novel 1, 4-dihydropyridine derivatives for certain pharmacological activities. *The Pharma Innovation* **6**, 165 (2017).
98. Gutiérrez-Bonet, A. L., Remeur, C., Matsui, J. K. & Molander, G. A. Late-stage C–H alkylation of heterocycles and 1, 4-quinones via oxidative homolysis of 1, 4-dihydropyridines. *J. Am. Chem. Soc.* **139**, 12251–12258 (2017).
99. Dehbalaei, M. G., Foroughifar, N., Pasdar, H. & Khajeh-Amiri, A. N-Propyl benzo guanamine sulfonic acid supported on magnetic Fe<sub>3</sub>O<sub>4</sub> nanoparticles: A novel and efficient magnetically heterogeneous catalyst for the synthesis of 1,8-dioxo-decahydroacridine derivatives. *New J. Chem.* **42**, 327–335 (2018).
100. Karhale, S., Patil, M., Rashinkar, G. & Helavi, V. Green and cost effective protocol for the synthesis of 1, 8-dioxo-octahydroxanthenes and 1, 8-dioxo-decahydroacridines by using sawdust sulphonic acid. *Res. Chem. Intermed.* **43**, 7073–7086 (2017).
101. Brinkerhoff, R. C. *et al.* Evaluation of the antioxidant activities of fatty polyhydroquinolines synthesized by Hantzsch multicomponent reactions. *RSC Adv.* **9**, 24688–24698. <https://doi.org/10.1039/C9RA04758A> (2019).
102. Gómez-Galeno, J. E. *et al.* b-annulated 1,4-dihydropyridines as Notch inhibitors. *Bioorg. Med. Chem. Lett.* **28**, 3363–3367. <https://doi.org/10.1016/j.bmcl.2018.09.002> (2018).
103. Nasr-Esfahani, M., Elhamifar, D., Amadeh, T. & Karimi, B. Periodic mesoporous organosilica with ionic-liquid framework supported manganese: an efficient and recyclable nanocatalyst for the unsymmetric Hantzsch reaction. *RSC Adv.* **5**, 13087–13094 (2015).
104. Pyrko, A. Synthesis and transformations of new 1, 2, 3, 4, 5, 6, 7, 8, 9, 10-decahydroacridine-1, 8-dione derivatives. *Russ. J. Org. Chem.* **44**, 1215 (2008).
105. Shchekotikhin, Y. M., Nikolaeva, T., Shub, G. & Kriven'ko, A. Synthesis and antimicrobial activity of substituted 1, 8-dioxodecahydroacridines. *Pharm. Chem. J.* **35**, 206–208 (2001).
106. Palermo, V. *et al.* First report about the use of micellar keggin heteropolyacids as catalysts in the green multicomponent synthesis of nifedipine derivatives. *Catal. Lett.* **146**, 1634–1647 (2016).
107. Janis, R. A. & Triggle, D. J. New developments in calcium ion channel antagonists. *J. Med. Chem.* **26**, 775–785. <https://doi.org/10.1021/jm00360a001> (1983).
108. Berkan, Ö. *et al.* Vasorelaxing properties of some phenylacridine type potassium channel openers in isolated rabbit thoracic arteries. *Eur. J. Med. Chem.* **37**, 519–523. [https://doi.org/10.1016/S0223-5234\(02\)01374-0](https://doi.org/10.1016/S0223-5234(02)01374-0) (2002).
109. Kidwai, M. & Bhatnagar, D. Ceric ammonium nitrate (CAN) catalyzed synthesis of N-substituted decahydroacridine-1, 8-diones in PEG. *Tetrahedron Lett.* **51**, 2700–2703 (2010).
110. Wainwright, M. Acridine—A neglected antibacterial chromophore. *J. Antimicrob. Chemother.* **47**, 1–13 (2001).
111. He, W., Ge, Y.-C. & Tan, C.-H. Halogen-bonding-induced hydrogen transfer to C=N bond with Hantzsch ester. *Org. Lett.* **16**, 3244–3247. <https://doi.org/10.1021/ol501259q> (2014).
112. Ghosh, S., Saikh, F., Das, J. & Pramanik, A. K. Hantzsch 1, 4-dihydropyridine synthesis in aqueous ethanol by visible light. *Tetrahedron Lett.* **54**, 58–62 (2013).
113. Dharma Rao, G. B., Nagakalyan, S. & Prasad, G. K. Solvent-free synthesis of polyhydroquinoline derivatives employing mesoporous vanadium ion doped titania nanoparticles as a robust heterogeneous catalyst via the Hantzsch reaction. *RSC Adv.* **7**, 3611–3616. <https://doi.org/10.1039/C6RA26664A> (2017).
114. Srinivasan, V. V., Pachamuthu, M. P. & Maheswari, R. Lewis acidic mesoporous Fe-TUD-1 as catalysts for synthesis of Hantzsch 1,4-dihydropyridine derivatives. *J. Porous Mater.* **22**, 1187–1194. <https://doi.org/10.1007/s10934-015-9995-8> (2015).
115. Zolfigol, M. A. & Yarie, M. Synthesis and characterization of novel silica-coated magnetic nanoparticles with tags of ionic liquid. Application in the synthesis of polyhydroquinolines. *RSC Adv.* **5**, 103617–103624. <https://doi.org/10.1039/C5RA23670C> (2015).
116. Ghorbani-Choghamarani, A., Rabiei, H., Tahmasbi, B., Ghasemi, B. & Mardi, F. Preparation of DSA@ MNPs and application as heterogeneous and recyclable nanocatalyst for oxidation of sulfides and oxidative coupling of thiols. *Res. Chem. Intermed.* **42**, 5723–5737 (2016).

117. Yaghoubi, A., Dekamin, M. G. & Karimi, B. Propylsulfonic acid-anchored isocyanurate-based periodic mesoporous organosilica (PMO-ICS-PrSO<sub>3</sub>H): A highly efficient and recoverable nanoporous catalyst for the one-pot synthesis of substituted polyhydroquinolines. *Catal. Lett.* **147**, 2656–2663 (2017).
118. Abdollahi-Alibeik, M. & Rezaeiipoor-Anari, A. Fe<sub>3</sub>O<sub>4</sub>@ B-MCM-41: A new magnetically recoverable nanostructured catalyst for the synthesis of polyhydroquinolines. *J. Magn. Magn. Mater.* **398**, 205–214 (2016).
119. Reddy, M. & Jeong, Y. T. Letter polystyrene-supported p-toluenesulfonic acid: A new, highly efficient, and recyclable catalyst for the synthesis of hydroxyridine derivatives under solvent-free conditions. *Synlett* **23**, 2985–2991 (2012).
120. Alirezvani, Z., Dekamin, M. G. & Valiey, E. New hydrogen-bond-enriched 1,3,5-tris(2-hydroxyethyl) isocyanurate covalently functionalized MCM-41: An efficient and recoverable hybrid catalyst for convenient synthesis of acridinedione derivatives. *ACS Omega* **4**, 20618–20633. <https://doi.org/10.1021/acsomega.9b02755> (2019).
121. Dekamin, M. G. *et al.* Alginic acid: A mild and renewable bifunctional heterogeneous biopolymeric organocatalyst for efficient and facile synthesis of polyhydroquinolines. *Int. J. Biol. Macromol.* **108**, 1273–1280. <https://doi.org/10.1016/j.ijbio.2017.11.050> (2018).
122. Dekamin, M. G. *et al.* Alginic acid: A highly efficient renewable and heterogeneous biopolymeric catalyst for one-pot synthesis of the Hantzsch 1,4-dihydropyridines. *RSC Adv.* **4**, 56658–56664. <https://doi.org/10.1039/C4RA11801D> (2014).
123. Kumar, R., Andhare, N. H., Shard, A. & Sinha, A. K. Multicomponent diversity-oriented synthesis of symmetrical and unsymmetrical 1,4-dihydropyridines in recyclable glycine nitrate (GlyNO<sub>3</sub>) ionic liquid: A mechanistic insight using Q-TOF ESI-MS/MS. *RSC Adv.* **4**, 19111–19121 (2014).
124. Davoodi, F., Dekamin, M. G. & Alirezvani, Z. A practical and highly efficient synthesis of densely functionalized nicotinonitrile derivatives catalyzed by zinc oxide-decorated superparamagnetic silica attached to graphene oxide nanocomposite. *Appl. Organomet. Chem.* **33**, e4735. <https://doi.org/10.1002/aoc.4735> (2019).
125. Dekamin, M. G., Ghanbari, M., Moghbeli, M. R., Barikani, M. & Javanshir, S. Fast and convenient synthesis of cross-linked poly(urethane-isocyanurate) in the presence of tetrabutylammonium phthalimide-N-oxyl or tetraethylammonium 2-(carbamoyl)benzoate as efficient metal-free cyclotrimerization catalysts. *Polym. Plast. Technol. Eng.* **52**, 1127–1132. <https://doi.org/10.1080/03602559.2013.779708> (2013).
126. Koçyiğit, S. *et al.* Structural investigation of boron undoped and doped indium stabilized bismuth oxide nanoceramic powders. *Ceram. Int.* **39**, 7767–7772 (2013).
127. Dekamin, M. G., Mehdipoor, F. & Yaghoubi, A. 1, 3, 5-Tris (2-hydroxyethyl) isocyanurate functionalized graphene oxide: a novel and efficient nanocatalyst for the one-pot synthesis of 3, 4-dihydropyrimidin-2 (1 H)-ones. *New J. Chem.* **41**, 6893–6901 (2017).
128. Liu, J., Shi, H., Shen, Q., Guo, C. & Zhao, G. A biomimetic photoelectrocatalyst of co-porphyrin combined with a g-C<sub>3</sub>N<sub>4</sub> nanosheet based on  $\pi$ - $\pi$  supramolecular interaction for high-efficiency CO<sub>2</sub> reduction in water medium. *Green Chem.* **19**, 5900–5910. <https://doi.org/10.1039/C7GC02657A> (2017).
129. Zarei, Z. & Akhlaghinia, B. Zn II doped and immobilized on functionalized magnetic hydroxalite (Fe<sub>3</sub>O<sub>4</sub>/HT-SMTU-Zn II): A novel, green and magnetically recyclable bifunctional nanocatalyst for the one-pot multi-component synthesis of acridinediones under solvent-free conditions. *New J. Chem.* **41**, 15485–15500 (2017).
130. Fekri, L. & Nikpassand, M. Benzyl alcohol-based synthesis of mono- and bis-dihydropyridines in the presence of Al(HSO<sub>4</sub>)<sub>3</sub>, sodium nitrite, and sodium bromide under solvent-free conditions. *Russ. J. Gen. Chem.* **86**, 1412–1418 (2016).
131. Rostamizadeh, S., Amirahmadi, A., Shadjou, N. & Amani, A. M. MCM-41-SO<sub>3</sub>H as a nanoreactor for the one-pot, solvent-free synthesis of 1, 8-dioxo-9-aryl decahydroacridines. *J. Heterocycl. Chem.* **49**, 111–115 (2012).
132. Bakibaev, A. A., Filimonov, V. & Nevzgodova, E. S. Ureas in organic synthesis VI. Reactions of 1,3-dicarbonyl compounds with azomethines and urea in dimethyl sulfoxide as a method for the synthesis of Aryl-substituted Acridine-1,8-diones and 1,4-dihydropyridines. *J. Org. Chem. USSR* **27**, 1332–1336 (1991).
133. Mahesh, P. *et al.* Magnetically separable recyclable nano-ferrite catalyst for the synthesis of acridinediones and their derivatives under solvent-free conditions. *Chem. Lett.* **44**, 1386–1388 (2015).
134. Ramesh, K. B. & Pasha, M. A. Study on one-pot four-component synthesis of 9-aryl-hexahydro-acridine-1,8-diones using SiO<sub>2</sub>-I as a new heterogeneous catalyst and their anticancer activity. *Bioorg. Med. Chem. Lett.* **24**, 3907–3913. <https://doi.org/10.1016/j.bmcl.2014.06.047> (2014).
135. Das, P., Dutta, A., Bhaumik, A. & Mukhopadhyay, C. Heterogeneous ditopic ZnFe<sub>2</sub>O<sub>4</sub> catalyzed synthesis of 4H-pyrans: Further conversion to 1,4-DHPs and report of functional group interconversion from amide to ester. *Green Chem.* **16**, 1426–1435 (2014).
136. Afsar, J., Zolfigol, M. A. & Khazaei, A. [Fe<sub>3</sub>O<sub>4</sub>@ SiO<sub>2</sub>@(CH<sub>2</sub>)<sub>3</sub>im] C6F5O as a new hydrophilic and task-specific nanomagnetic catalyst: Application for synthesis of  $\beta$ -azido alcohols and thiiranes under mild and green conditions. *ChemistrySelect* **3**, 11134–11140 (2018).
137. Nasresfahani, Z. & Kassaee, M. Mesoporous silica nanoparticles in an efficient, solvent-free, green synthesis of acridinediones. *Catal. Commun.* **60**, 100–104 (2015).
138. Suárez, M., Loupy, A., Salfrán, E., Morán, L. & Rolando, E. Synthesis of decahydroacridines under microwaves using ammonium acetate supported on alumina. *Heterocycles* **51**, 21–27. <https://doi.org/10.3987/COM-98-8272> (1999).
139. Goli-Jolodar, O., Shirini, F. & Seddighi, M. Introduction of a novel nanosized N-sulfonated Brønsted acidic catalyst for the promotion of the synthesis of polyhydroquinoline derivatives via Hantzsch condensation under solvent-free conditions. *RSC Adv.* **6**, 26026–26037 (2016).
140. Gazerani, P. G. *et al.* Magnetite polycitric acid (Fe<sub>3</sub>O<sub>4</sub>@ PCA) nanoparticles: A novel, efficient and reusable solid acid catalyst for the preparation of polyhydroquinolines. *Lett. Org. Chem.* **14**, 787–796 (2017).
141. Yarhosseini, M., Javanshir, S., Dekamin, M. G. & Farhadnia, M. Tetraethylammonium 2-(carbamoyl) benzoate as a bifunctional organocatalyst for one-pot synthesis of Hantzsch 1, 4-dihydropyridine and polyhydroquinoline derivatives. *Monatsh. Chem.* **147**, 1779–1787 (2016).
142. Li, B. L., Zhong, A. G. & Ying, A. G. Novel SO<sub>3</sub>H-functionalized ionic liquids-catalyzed facile and efficient synthesis of polyhydroquinoline derivatives via hantzsch condensation under ultrasound irradiation. *J. Heterocycl. Chem.* **52**, 445–449 (2015).
143. Sakram, B., Sonyanaik, B., Ashok, K. & Rambabu, S. Polyhydroquinolines: 1-sulfofpyridinium chloride catalyzed an efficient one-pot multicomponent synthesis via Hantzsch condensation under solvent-free conditions. *Res. Chem. Intermed.* **42**, 7651–7658 (2016).
144. Tajbakhsh, M., Alinezhad, H., Norouzi, M., Bagheri, S. & Akbari, M. Protic pyridinium ionic liquid as a green and highly efficient catalyst for the synthesis of polyhydroquinoline derivatives via Hantzsch condensation in water. *J. Mol. Liq.* **177**, 44–48 (2013).
145. Davoodnia, A., Khashi, M. & Tavakoli-Hoseini, N. Tetrabutylammonium hexatungstate [TBA]<sub>2</sub>[W<sub>6</sub>O<sub>19</sub>]: Novel and reusable heterogeneous catalyst for rapid solvent-free synthesis of polyhydroquinoline via unsymmetrical Hantzsch reaction. *Chin. J. Catal.* **34**, 1173–1178 (2013).
146. Yü, S.-J., Wu, S., Zhao, X.-M. & Lü, C.-W. Green and efficient synthesis of acridine-1, 8-diones and hexahydroquinolines via a KH<sub>2</sub>PO<sub>4</sub> catalyzed Hantzsch-type reaction in aqueous ethanol. *Res. Chem. Intermed.* **43**, 3121–3130 (2017).
147. Ghorbani-Vaghei, R., Malaekhepoor, S. M., Hasanein, P., Karamyan, R. & Asadbegy, M. Synthesis and biological evaluation of new series 1, 4-dihydropyridines. *Res. Chem. Intermed.* **42**, 4715–4731 (2016).
148. Faisal, M. *et al.* DABCO-PEG ionic liquid-based synthesis of acridine analogues and its inhibitory activity on alkaline phosphatase. *Synth. Commun.* **48**, 462–472 (2018).

149. Rashedian, F., Saberi, D. & Niknam, K. Silica-bonded N-propyl sulfamic acid: A recyclable catalyst for the synthesis of 1, 8-dioxo-decahydroacridines, 1, 8-dioxo-octahydroxanthenes and quinoxalines. *J. Chin. Chem. Soc.* **57**, 998–1006 (2010).
150. Karade, N. N., Budhewar, V. H., Shinde, S. V. & Jadhav, W. N. L-proline as an efficient organo-catalyst for the synthesis of polyhydroquinoline via multicomponent Hantzsch reaction. *Lett. Org. Chem.* **4**, 16–19 (2007).
151. Wang, L.-M. *et al.* Facile Yb(OTf)<sub>3</sub> promoted one-pot synthesis of polyhydroquinoline derivatives through Hantzsch reaction. *Tetrahedron* **61**, 1539–1543 (2005).
152. Cherkupally, S. R. & Mekala, R. *P*-TSA catalyzed facile and efficient synthesis of polyhydroquinoline derivatives through Hantzsch multi-component condensation. *Chem. Pharm. Bull.* **56**, 1002–1004. <https://doi.org/10.1248/cpb.56.1002> (2008).
153. Mobinikhaledi, A. *et al.* Efficient one-pot synthesis of polyhydroquinoline derivatives using silica sulfuric acid as a heterogeneous and reusable catalyst under conventional heating and energy-saving microwave irradiation. *Synth. Commun.* **39**, 1166–1174 (2009).

## Acknowledgements

We are grateful for the financial support from The Research Council of Iran University of Science and Technology (IUST), Tehran, Iran (Grant No 160/19108). We would also like to acknowledge the support of The Iran Nanotechnology Initiative Council (INIC), Iran.

## Author contributions

M.S. worked on the topic as her MSc. Thesis and prepared the initial draft of the manuscript. Prof. M.G.D. is the supervisor of Sam and Z.A. as his MSc. and Ph.D. students, respectively. Also, he edited and revised the manuscript completely. Z.A. worked closely with Miss Sam for doing experimental section and interpretation of the characterization data of both catalyst and products.

## Competing interests

The authors declare no competing interests.

## Additional information

**Supplementary Information** The online version contains supplementary material available at <https://doi.org/10.1038/s41598-020-80884-z>.

**Correspondence** and requests for materials should be addressed to M.G.D.

**Reprints and permissions information** is available at [www.nature.com/reprints](http://www.nature.com/reprints).

**Publisher's note** Springer Nature remains neutral with regard to jurisdictional claims in published maps and institutional affiliations.



**Open Access** This article is licensed under a Creative Commons Attribution 4.0 International License, which permits use, sharing, adaptation, distribution and reproduction in any medium or format, as long as you give appropriate credit to the original author(s) and the source, provide a link to the Creative Commons licence, and indicate if changes were made. The images or other third party material in this article are included in the article's Creative Commons licence, unless indicated otherwise in a credit line to the material. If material is not included in the article's Creative Commons licence and your intended use is not permitted by statutory regulation or exceeds the permitted use, you will need to obtain permission directly from the copyright holder. To view a copy of this licence, visit <http://creativecommons.org/licenses/by/4.0/>.

© The Author(s) 2021